Compact coherent backlight illuminator for wide field-of-view near to eye displays

by

Hazal ER

A Thesis Submitted to the
Graduate School of Sciences and Engineering
in Partial Fulfillment of the Requirements for
the Degree of

Master of Science
in
Electrical & Electronics Engineering

Koc University

October 2016

Koc University

Graduate School of Sciences and Engineering

This is to certify that I have examined this copy of a master's thesis by

Hazal Er

and have found that it is complete and satisfactory in all respects,

and that any and all revisions required by the final

examining committee have been made.

Committee Members:

____

Prof. Dr. Hakan Ürey, (Koç University, Advisor)

____

Assoc. Prof. Dr. Göksenin Yaralıoğlu (Özyeğin University)

____

Asst. Prof. Dr.Fehmi Çivitçi, (İTÜ)

Date: 13.10.2016

ABSTRACT

The advancements in micro-electronics, optics and fabrication during the recent decades have led to an ever rising miniaturization, personalization and mobility trend in technology. Just as the headphones that replaced loudspeakers; large televisions and monitors are getting substituted by personal and portable displays, including the wearable near to eye displays (NEDs). Immersive NEDs present users virtual reality (VR), while optically see-through NEDs present augmented reality (AR), with dozens of niche applications in entertainment, education, medical and military domains. The ultimate NED should simultaneously provide high resolution, wide field-of-view (FOV), thin form-factor, large eye box, sufficient brightness and light efficiency, which are all competing requirements. Existing solutions indeed meet merely a subset but not all of the listed objectives.

In this thesis, a novel fiber based point source illuminator for near to eye displays capable of presenting wide field of view is presented. The proposed technology is suitable for both immersive (virtual reality) and optical see-through (augmented reality) applications. Proposed design is a coherent backlight illuminator that combines a fiber, scattering nanoparticles and a concave or ellipsoidal mirror which converts the wave from fiber to a converging wave. It is also possible to minimize the volume and to use the demonstrated technology in equipment where small form factor is important. The technology is also adjustable for different illumination profiles (collimated, converging, diverging etc.). Point source fabrication and three different configurations for point source usage are presented. Images captured with a computer generated holograms are presented to support the validity of the design.

ÖZET

Geçtiğimiz yıllarda mikro-elektronik, optik ve üretim alanında yaşanan ilerlemeler teknolojide minyatürleşme, kişiselleşme ve mobilleşme eğilimini de beraberinde getirdi. Hoparlörlerin yerini kulaklıklara bırakması gibi, büyük ekranlar da yerini taşınabilir olan alternatiflerine bırakmaya başladı. Günümüzde sanal gerçeklik ve artırılmış gerçeklik sunan gözlükler eğlence, eğitim, tıp ve askeri alanlarda sıkça kullanım bulmaktadır. Bu akıllı gözlüklerde beklenen özellikler yüksek çözünürlükte görüntü vermeleri, yüksek görme alanına sahip olmaları, taşınabilir ve hafif olmaları, yeterli parlaklıkta aydınlatmaya sahip olmalarıdır. Halihazırda var olan ürünler bu sıralanan özelliklerden yalnızca bir ya da birkaçına sahiptir.

Bu tez çalışmasında akıllı gözlüklerde kullanılmak üzere geniş görme alanı yaratabilen, kompakt coherent arka ışık kaynağı tasarımı yapılmıştır. Bu ışık kaynağı, bir fiberin ucuna ışığın dağılmasını sağlayacak nano parçacıklar konularak tasarlanmıştır. Sistem içbükey aynalarla tamamlanarak ışığın yakınsak bir profile kavuşması sağlanmıştır. Tasarlanan ışık kaynağı iletici veya yansıtıcı ekranlarda, sanal ve artırılmış gerçeklik gözlüklerinde, uzaysal ışık modülasyonu ile 3 boyutlu holografik sistemlerde kullanılabilmektedir.

ACKNOWLEDGEMENTS

I would like to express my sincere gratitude to my advisor Prof. Dr. Hakan Ürey. He was my advisor starting from my sophomore year, and he is supporting me ever since that time. I would like to thank him for accepting me as a graduate student at Optical Microsystems Laboratory, and believing in me. It was a privilege for me to work in such an important project under his supervision. I also thank him for his expert advice, guidance with his immense knowledge, patience and encouragement. I always feel myself comfortable when I want to consult him about my career plans after Master degree. I cannot imagine a better advisor.

I gratefully acknowledge the member of my thesis committee Assoc. Prof. Dr. Göksenin Yaralıoğlu for his valuable participation and insights.

I would like to thank Asst. Prof. Dr. Fehmi Çivitçi for guiding my research and his best suggestions, thanks to his great ability to explain complex ideas in simple terms, things always become simpler. I know that without his patient and help it will be undoubtedly more difficult to completing this work.

I would also like to thank Erdem Ulusoy, who is always willing to help, for allowing to use his mask design. His guidance after I started to work was really priceless. He encouraged me when I feel desperate. Words cannot express how I feel grateful to Erdem Ulusoy.

My sincere thanks also go to Sven Holmstrom who taught me how to use white light interferometer and index matching, Muhsin Eralp who helped me a lot with ZEMAX and Selim Ölçer who knows the answer of every question about lab. I would also like to thank all OML members for their friendship and collaboration.

I gratefully acknowledge Vehbi Koç Foundation for establishing such an excellent university in our country and give us the chance to take good education. I also want to thank my managers in Arçelik. During final part of my thesis work, I had to manage both work and school for a while. I appreciate their understanding and support.

I would like to say a heartfelt thank you to my mum Mücella, my dad Şemsi, my sister Balam and my brother Can for their constant love and support, my friends Tuğçe and Irmak for their close friendship beginning from the first day of my university life, my old flatmate Bengisu for her sincerity. I would like to express my deep sense of gratitude toward them.

And lastly my endless thanks go to Mustafa Kemal Atatürk for bringing secularism and equal rights as well as believing in Turkish women and supporting them.

I dedicated my thesis to my parents who have given me the opportunity to start Koç University for my Bachelor degree, and encouraged me to continue for a master degree.

TABLE OF CONTENTS

LIST OF FIGURES

ABBREVIATIONS

3D…………………………………………………………………………...3 dimensional

ABS…………………………………………………………Acrylonitrile Butadiene Styrene

AFM…………………………………………………………Atomic Force Microscopy

AR…………………………………………………………………….Augmented Reality

CBI……………………………………………………….. Coherent backlight illuminator

CGH……………………………………………………… Computer Generated Hologram

CNC…………………………………………………………Computer numerical control

DOE…………………………………………………………Diffractive optical elements

EPE…………………………………………………………………Exit pupil expander

FOV…………………………………………………………………….Field of view

HMD………………………………………………………….. Head mounted display

LCoS………………………………………………………….Liquid Crystal on Silicon

LED…………………………………………………………………. Light emitting diode

MEK…………………………………………………………………Methyl ethyl ketone

NA…………………………………………………………………….Numerical Aperture

NED…………………………………………………………...Near to eye display

PVC……………………………………………………………………Polyvinyl chloride

SLM……………………………………………………...… Spatial Light Modulator

TiO_2…………………………………………………………………Titanium dioxide

TIR……………………………………………………………Total Internal Reflection

UV……………………………………………………………………………. Ultra violet

VR…………………………………………………………………………Virtual reality

ZnO………………………………………………………………………..Zinc oxide

1. INTRODUCTION

Recently, there has been a trend of evolution of media from large to small and personal. Headphones took the place of loudspeakers and with the new trend big displays are evolving to personal and smaller ones. Near to eye displays can be considered as the headphones of the display world since they are small and portable, and allow personal viewing experiences.

Figure 1: Evolution of media from large and shared to small and personal [1].

Near to eye display (NED), also known as head mounted displays (HMD), is a wearable display which allows its user to experience watching 2D or 3D content by creating a display in front of user's field of vision.

NEDs are divided into two categories: Immersive NEDs and optically see-through NEDs. While immersive displays present user a *virtual reality* (VR), optically see-through displays present *augmented reality* (AR). An immersive display immerses the user an artificial environment which is generated by software, whereas see-through displays blend real world and virtual computer generated information [2].

Figure 2: The categorization of NEDs [1].

Immersive and see-through NEDs are also divided into two as shown in Figure 2. For cinema glasses, the FOV changes between 30-60° and is 90+° for virtual reality displays. However, AR headsets have 20-60° FOV. Smart glasses, such as Google Glass, have smaller FOV values and smart glass users do not look through the display continuously; they look at the display periodically [1].

Although virtual reality and augmented reality terms seem to have just appeared, their origins reach back five decades. Morton Heilin, a cinematographer, who invented Sensorama in 1957, is known as the leader of virtual reality [3]. Sensorama is the first appearance of virtual reality and was patented in 1960 [3]. The device combined projected film with audio, vibration, wind and odors for users to feel as if they were actually in the film. Figure 3 shows a side view of Heilin's invention in the patent application in 28 August 1962.

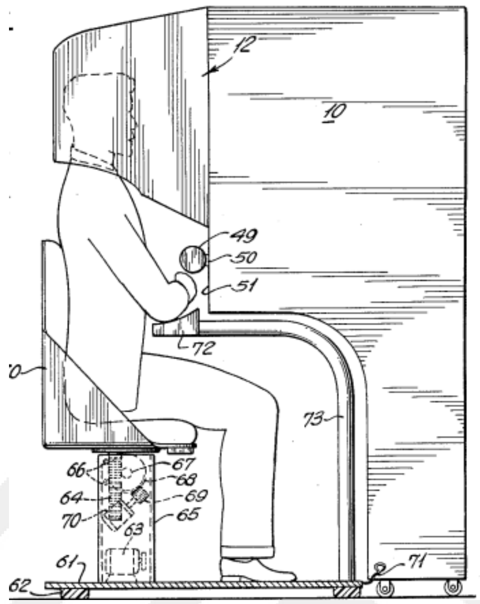

Figure 3: The Sensorama [4].

In 1968, Ivan Sutherland demonstrated the world's first optical-see through head-mounted eyepiece display. Sutherland's invention is named the "Sword of Damocles" due to its tremendous appearance. Sword of Damocles is a Greek legend about Dionysius, the king of Syracusan, and his friend Damocles, who was fawning over the king, trying to curry favor. Dionysus switches places with Damocles to teach him a lesson. While Damocles sat in the king's throne surrounded by luxury, he realized that a sharp sword was hanging over his head which was tied by a single horse hair to demonstrate the precariousness of a king's fortune. Since Sutherland's device was also suspended from the ceiling as it was too heavy to be worn it got its name from this legend. Figure 4 shows Sutherland's Sword of Damocles.

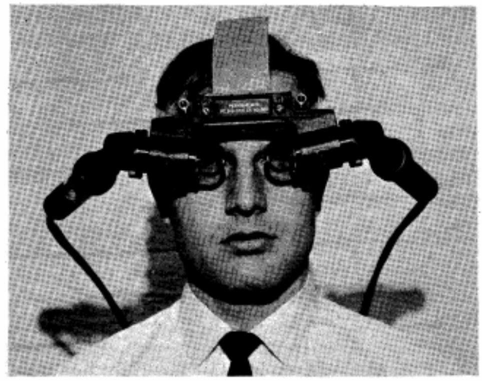

Figure 4: Ivan Sutherland's Sword of Damocles [5].

Sutherland’s invention inspired other research and paved the way for further devices. With Sutherland’s pioneering work, great advances in near to eye display technologies have since been made by researchers. Figure 5 shows 45 years of digital eyewear after Sutherland’s invention. These smart glasses are on display at the Augmented Reality Expo.

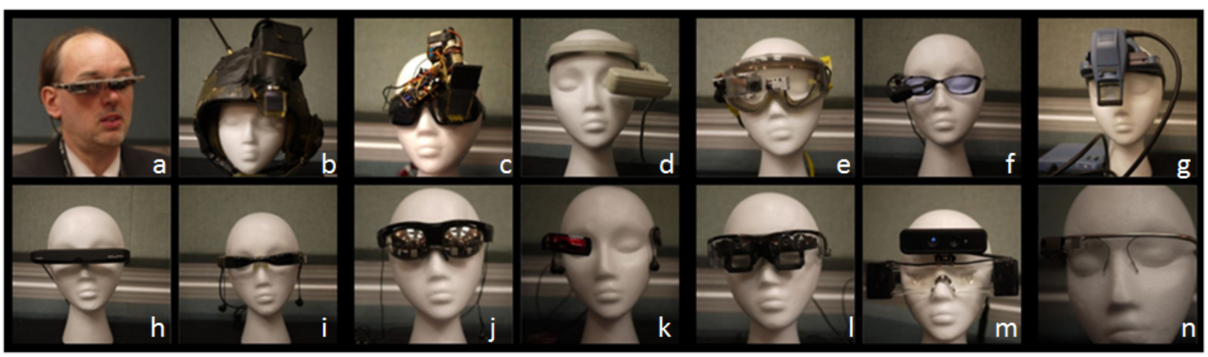

Figure 5: Evolution of digital eyewear from 1968 through 2013 a) Steve Mann with EyeTap Digital Eye Glass b) 1980: Steve Mann's WearComp1 c) 1984: Steve Mann's WearComp 4 d) 1989: Reflection Technology's The Private Eye e) 1998: Digital Eye Glass EyeTap Augmediated Reality Goggles f) 2000:MicroOptical's TASK-9 g) 2005: MicroVision's Nomad Digital Displayh) 2005: Vuzix V920 i) 2008: MyVu Personal Media Viewer, Crystal Edition j)2009: Vuzix Wrap SeeThru Proto k) 2010: VISCOM l) 2011: Vuzix WrapAR 920 m)2013: Meta prototype for developers n)2013: Google Glass [6].

The angle of visible display from the user's perspective is named field of view (FOV), and is one of the most important parameters for displays. The greater the FOV, the better the display is, because it provides a greater sense of immersion. The FOV of the human eye is 200° as a result of overlap of 130° with 120° [7].

Occulus Rift and Gear VR are two of the commercial virtual reality products that have approximately 100° FOV [8]. See-through NED is gradually becoming very popular with numerous potential applications; e.g., it can be used for military, entertainment, education and medical applications [9].

FOV values of some commercial optical see-through NEDs are as follows: Google Glass has about 15° diagonal FOV [10]. Vuzix has different products for see-through augmented reality NEDS. STAR 1200XLD has 35°, M2000AR has 30° and Wrap 1200DXAR has 35° diagonal FOV [11].

Currently, near to eye displays are popular and have numerous potential applications. To be of practical utility, a near to eye display should have wide FOV with simple optical elements; however, emerging devices have solutions only for one of these restrictive problems. They can provide either high FOV or light-weight products [13].

Innovega gives a technology comparison table that shows the relation between bulkiness and FOV values of commercial head mounted displays.

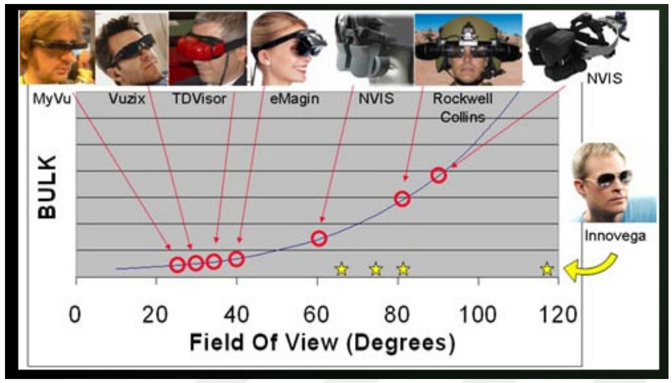

Figure 6: Technology comparison table [12].

With this study, our commitment is that we can make a backlight illuminator for a NED which can be transparent and has a wide FOV and as natural as wearing a pair of eyeglasses which can provide natural looking and interactive 3D.

The thesis is organized as follows: Chapter 2 provides necessary background information and a literature review on studies on NEDs. Chapter 3 explains the fabrication flow of our novel compact coherent backlight illuminator (CBI) for wide field-of-view (FOV) near-to-eye displays (NEDs). We present three experimental prototypes. The first is a proof-of-concept non-compact design that uses an off the shelf large radius spherical concave mirror. The second prototype is a compact design in which we manufacture a low f-number concave mirror by covering the curved surface of an off the shelf plane convex lens with a semi-transparent chromium layer. The third prototype uses an ellipsoidal mirror we designed and was fabricated by a company via diamond turning. Chapter 4 gives a summary on experimental results.

1.1 Contributions of the Thesis

The main contribution of this thesis is in the design of a compact coherent backlight illuminator (CBI) for wide field-of-view (FOV) near-to-eye displays (NEDs). It is not possible for light to scatter such a short distance with conventional methods. In the proposed CBI design, this problem is remedied by using scattering nanoparticles at the tip of the fiber, hence a 180 degree illumination is achieved with proposed Point Light Source (PLS).

We show three experimental prototypes to verify the design. After proof-of-concept non-compact design via coating a plano convex lens with chromium a semi-transparent compact solution is achieved. PLS is also embedded into a transparent, indexed match carrier rod via epoxy based attachment. In the third prototype, an ellipsoidal mirror is used to solve spherical aberration problems. Zemax simulations are conducted to prove the convergence of light; images are taken with CGHs to verify the premises of the design. The final design has a FOV of 70 degrees.

Traditional coherent wave generators are mainly on axis configurations consisting of multi-mode fibers (without nanoparticles at the tip as proposed design) and a lens. The light coming out of the fiber and passing through the lens requires at least 10 cm distance to propagate. For a 5 cm lens aperture, the approximate volume will be 250 cm^3 (5 cm * 5 cm * 10cm). Due to increased refraction of light rays when they strike at the edge of the lens, it is impossible for all incoming rays to focus in the same focal point. This effect ends up with a reduction in FOV. An average FOV with conventional systems can give a FOV of 50 degrees. The volume becomes about 50 cm^3 (2 cm * 5 cm * 5 cm) in the proposed design with an ellipsoid mirror, which is an improvement in size by 5 times and an increase in FOV by 40%.

A manuscript containing the studies in this thesis will be submitted to Optics Express.

2. LITERATURE REVIEW

2.1 Conventional NED Designs

Engineers in Nokia Research Center, Nokia's industrial research unit, have conducted several studies on near to eye displays.

T.Järvenpää and V.Aaltonen summarize the most timely NED concept as in Figure 7. The image coming from the image source is enlarged with optics and the virtual image is seen by the user at a certain distance. The drawbacks of these former NED designs are heaviness and the block on user's vision. Järvenpää et al. suggest using holography or diffractive optical elements (DOE) on planar waveguides [14].

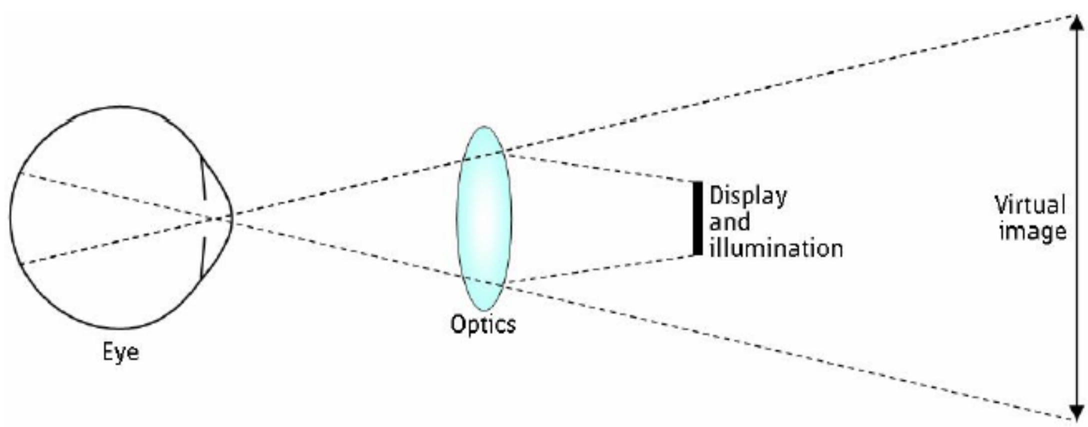

Figure 7: Basic NED concept [14].

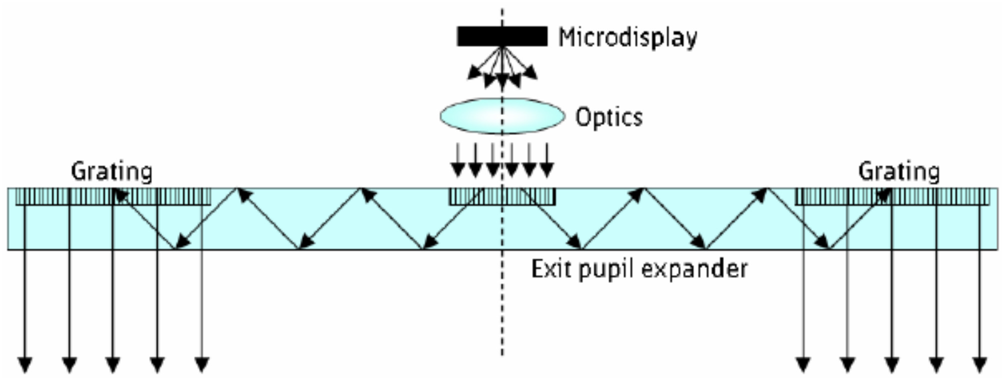

Figure 8: Gratings in Järvenpää's design [14].

The image source sends light in the middle of the plate. The light couples in from the middle of the plate and splits to two directions. The place where the light comes into the plate is called the in-coupling area whereas the two places where the light goes outside of the plate through eyes are called out-coupling areas. The gratings in the in-coupling part allow the beams to be divided into two and propagate in reverse directions

Figure 8 and Figure 9 show Järvenpää's design with exit pupil expanders (EPE). Images from the display are transferred to the eyes via transparent light guides. The reason behind the design in a chevron angle is to reduce distracting external reflections [14]. Since light guides are based on diffraction and the grating changes depending on the wavelength of the light, two different plates were used for each eye. One is for red and the other is for blue and green [14,15].

With the transparency feature of the light guides it is possible for the user to see both the real environment and the virtual images on top of it. Figure 10 shows the view of the test room before and after using their NED prototype and Figure 11 shows the NED prototype itself.

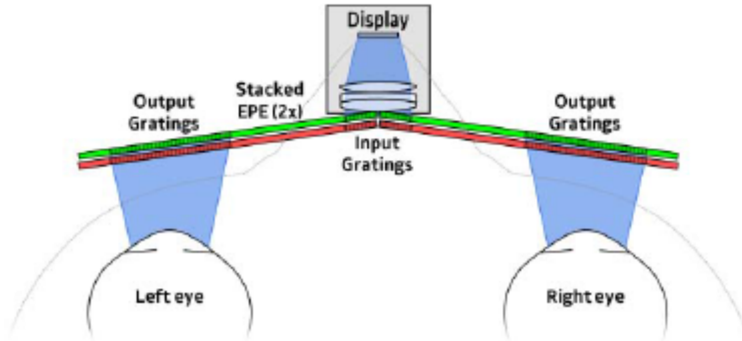

Figure 9: Light is transmitted from the display to both eyes through transparent EPE plates[15].

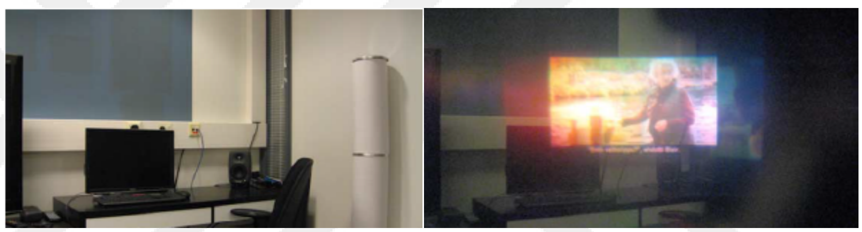

Figure 10: a)View of the room b) View through of the proposed NED prototype by Nokia Research Center [15].

Figure 11: The NED prototype of Nokia Research Center [15].

Diffractive waveguide technology, proposed by the Nokia Research Center is licensed by Vuzix. Although in the near to eye display world, Google Glass is a well-known product, Microsoft and Apple have also patented their own technology. There are lesser known players such as Optinvent, Epson Moverio, Atheer One, Recon Ret, Meta spaceglasses, Weon Glasses, Chipsip, Laforge Optical, Epiphany Eyewear, Kopin, Sony smart glass, Lumus DK40, Lenova smart glass, Xoeye Technologies, Innovega iOptik and 4II SportIIII [16].

Andrew Maimone, PhD student of Prof. Henry Fuchs along with researchers from Nvidia Research and University of North Carolina have been working on developing a new kind of AR device that consists of an LCD panel and an array of point light sources implemented as an edge-lit, etched acrylic sheet. The point sources in Maimone's design are placed directly in front of the eye out of focus. The point light sources are coded through the LCD to form miniature see-through projectors.

Conventional augmented reality glasses are bulky due to their complex optical components such as lenses, beam splitters, waveguides, reflectors etc. The other limitation of conventional AR glasses is their limited FOV.

Maimone's Pinlight Display replaces conventional optical components with an array of bright dots dubbed pinlights. Light rays appear in focus without the use of lenses because they hit each display pixel come from the same direction. Although Maimone's prototype achieves a 110 degree diagonal FOV which can make a huge difference in the viewing experience and has a compact design compared to conventional AR glasses, it also exhibits several limitations. The current system does not contain pupil tracking although it is strictly required. The other limitation is the image quality limitation due to the diffraction. Low cost LCD spatial light modulator usage dims the brightness of the environment like sunglasses. The prototype also suffers from low resolution compared with the existing commercial AR glasses [17].

Figure 12: Maimone's Pinlight Display prototype [17].

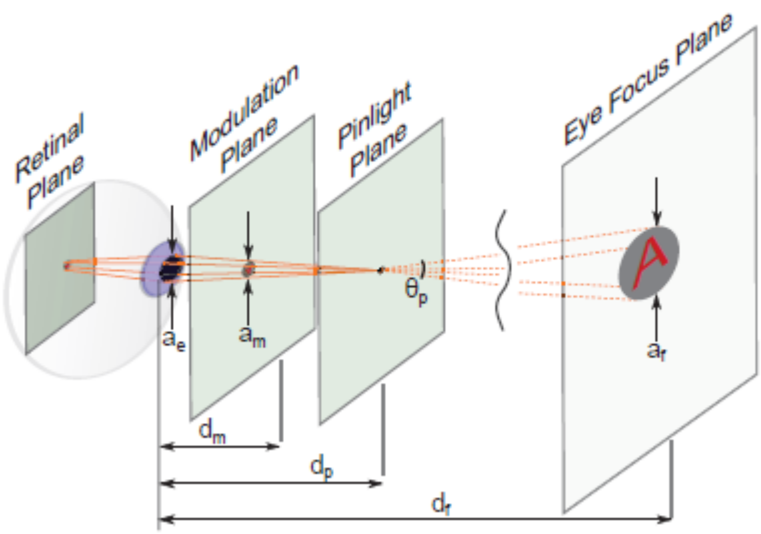

Figure 13: Pinlight Projection [17].

Light from a defocused point source is projected into the eye while being encoded with an SLM. In spite of the hardware components' out of focus stand, the focused image is formed on the retina without the use of any lenses.

Maimone et al. calculated the FOV through the single pinlight of their proposed system θ_p as in Equation (2.1) [4]

$$\theta_p = 2tan^{-1}\left(\frac{a_e}{2d_p}\right) \quad (2.1)$$

where a_e is the given aperture diameter and d_p is the pinlight distance.

See-through capability is provided/preserved using transparent components: a transmissive SLM and see-through point light array. Hence, a bulky design is prevented.

The other new technology is called IOptik. The human eye is limited to focus on objects very near to it. The objects that are very near to the human eye become blurred. This limitation inspired engineers to develop complex optical designs. Innovega suggests an alternative display technology that upgrades human eye capabilities. With their IOptik design they eliminate bulky optics and improve the sharpness of user's real world vision [18]. iOptik's special lens design will allow the human eye to focus on both close and far away objects. iOptik lenses must be paired with Innovega's glasses that contain micro-projectors. Figure 14 shows iOptik special lens. This contact lens works as a filter. While ambient light from the environment can pass through the outer filter, the center filter part blocks its transition. Figure 15 shows how ambient light and the light coming from the display pass through iOptik lens. However, it is unknown if there is a long term negative effect on human eye health.

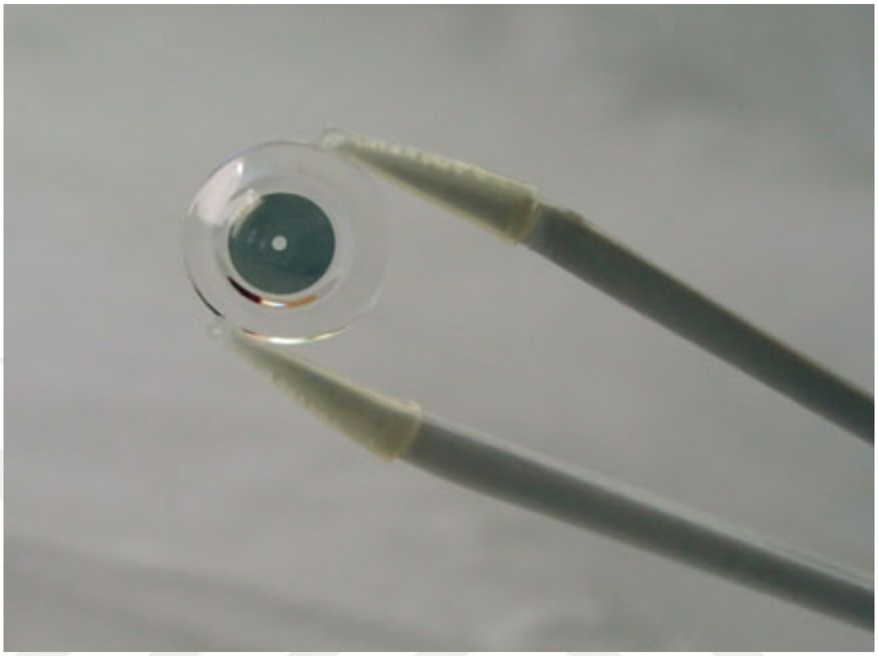

Figure 14: iOptik augmented reality prototype [18].

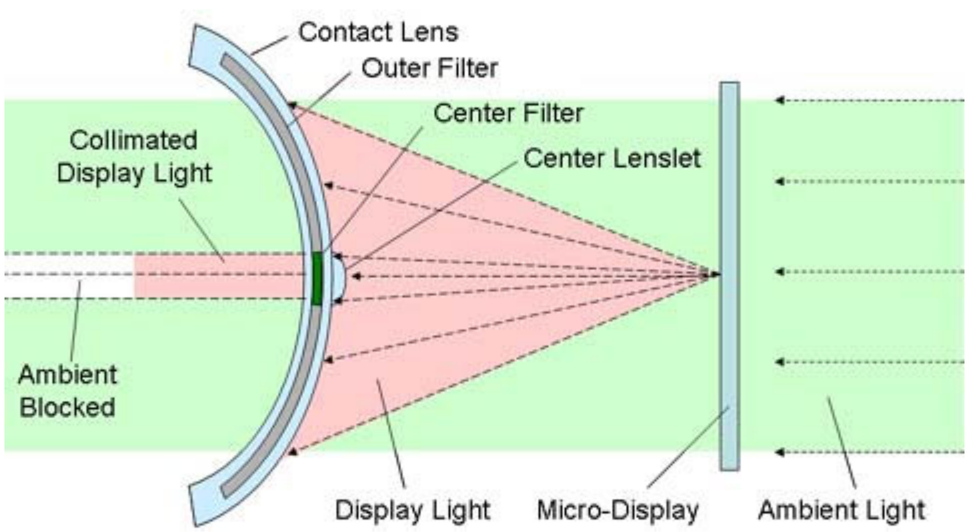

Figure 15: iOptik lens works as a filter [18].

2.2 Available coherent backlight or directional backlight solutions

Holographic 3D displays have recently become a popular topic. FOV is the angular extent of a given scene on display and an important parameter for displays.

LCD screens (monitors, TVs) have a wide FOV because they have a backlight consisting of a diffused light source at the back of the panel. However, the phase of the propagating waves becomes randomized, and it is not suitable to use with holographic reconstructions. 3D image formation with holographic reconstructions is based on light interference and requires coherence [19].

The other important parameter in backlight unit design for displays is minimizing the thickness. So far there have been only a few attempts to build thin BLU designs for holographic displays; most systems have bulky BLUs. Minimizing backlight thickness will result in a reduced overall thickness of the display [20].

In conventional holographic 3D display systems, the backlight units consist mainly of lenses and spatial filters with the purpose to improve both the coherence of LED light source and expand laser beam to a proper size [21]. It is possible to use both laser and LED as light sources with holographic 3D display systems. However, a spatial filter is mostly needed to improve the spatial coherence of the LED light source [21].

Chil-Sung Choi et al. proposed an ultra-slim coherent backlight unit which can be used for mobile holographic display. Their system consists of glass substrate for waveguide and two surface gratings produced by two-beam interference. The purpose of using two gratings is to solve chromatism. One surface grating has chromatical aberration and is cancelled by the output grating [20].

Figure 16 shows the fabrication procedures of the backlight unit and Figure 17 shows a photograph of the backlight unit Chil-Sung Choi et al. proposed.

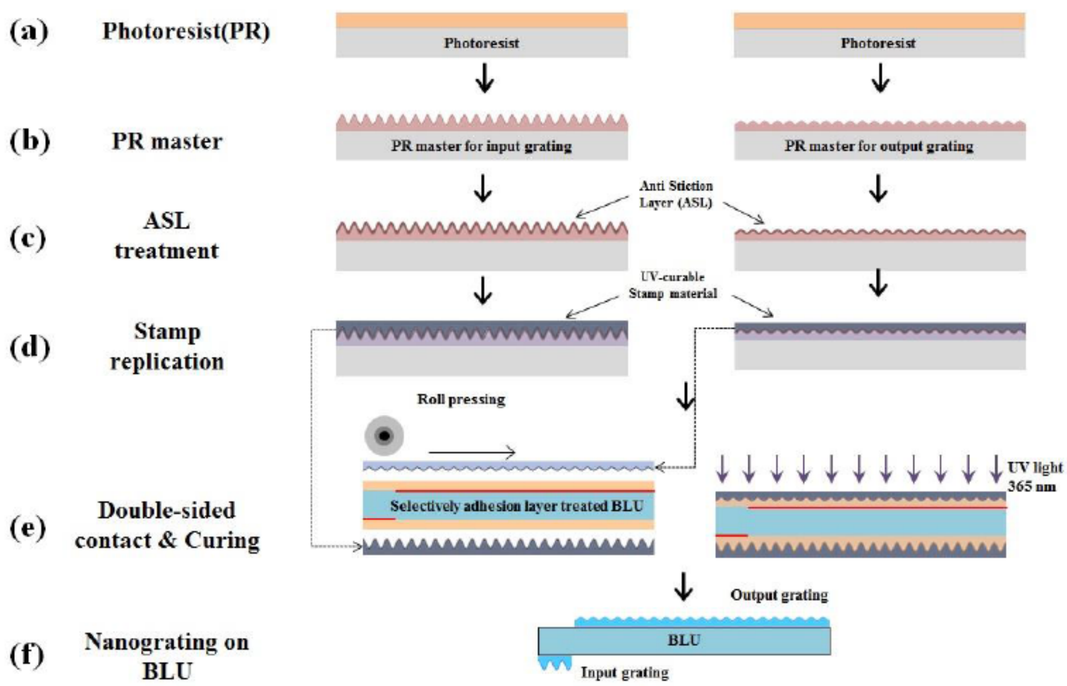

Figure 16: Process flow for fabricating a slim backlight unit [20].

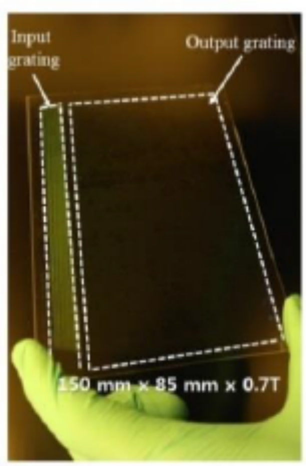

Figure 17: Photograph of slim coherent backlight unit [20].

The other study proposing coherent backlight system for flat-panel holographic 3D display was conducted by Yuan Xiong et al. [21]. Previously recorded reflection hologram was used in place of a conventional beam expander to convert the scattered laser input while obtaining a large scale coherent plane wave output. The reason behind the necessity of using a beam expander is to expand the collimated laser beam so that it can illuminate the whole required region of SLM. However, conventional beam expanders composed of a telescope configuration of two lenses along a common axis need noticeable optical length which is not suitable for flat panels. There are a few compact expanders [22, 23]. However, these compact expanders use the optical folding method, and this method only helps to shorten optical length only in one dimension. The other disadvantage of this method is that it still needs additional space for the folded optical path and limits the aperture ratio of the whole device.

However, Yuan Xiong et al. proposed a different compact holographic expander. The researchers used an expander with a diffuser to scatter the incident light into a large area. A reflection hologram previously recorded is then used to reshape the scattered light field into a coherent one.

Spatial coherence is defined as the capability of various object points to interfere with each other and is essential to recording holograms [24]. However, Stroke and Funkhouser indicated a possibility which creates an exception. They recorded a spectroscopic Fouriertransform hologram with spectrally non coherent light, in a two-beam Michelson Twyman-Green interferometer, and used it to produce spectra directly by a second Fourier transformation in the focal plane of a lens. [24]. Afterwards E.N. Leith discussed noncoherent light usage, however no results have been shared [24].

Byung Jin Chang has also demonstrated a holographic reconstruction with non-coherent light. The source he used was “continuous-spectrum white light zirconium arc source”. He used diffraction gratings as beam splitters and beam deflectors. By this means easy control of the modulation transfer function was achieved by changing the position of gratings or recording plane so that low pass, band pass or high pass characteristics were produced [25].

The above designs are FOV limited. The advantage of the proposed design in this thesis is high FOV, as it is compatible with multicolor and is easily fabricated.

3. BACKLIGHT ILLUMINATOR DESIGN

3.1.Introduction

The purpose of this thesis is to present a fiber based point source illuminator for optical see-through near to eye displays capable of presenting wide FOV. The proposed technology is suitable for augmented reality applications. The proposed design combines a fiber, scattering nanoparticles and a concave mirror. It is also possible to minimize the volume and use the demonstrated technology in equipment where a small form factor is important. The technology is also adjustable for different illumination profiles (collimated, converging, diverging etc.).

The path along which light travels is called a *ray* and a bundle of ray is a *beam of light*. There are mainly three types of beams:

1-Parallel Beams: When light rays travel parallel to each other, they are called parallel beams.

2-Divergent Beams: When light rays start from a point and travel in various directions, they are called divergent beams.

3-Converging Beams: When light rays coming from different direction meet at a point they are called converging beams.

The CGH mask we used in our experiments requires using converging light, so we positioned the CGH mask at a location before the reflecting beams focuses at a point.

Point source fabrication and two different configurations for point source usage are explained and simulation results are presented to support the validity of the design.

3.2 Fabrication of Fiber Based Point Source

3.2.1. Theory

Optical fibers are transparent, flexible, glass or plastic transmission channels that transmit light between the two ends. They work according to the total internal reflection principle (TIR). The first experimental demonstration of guiding of light by TIR was first demonstrated by Daniel Colladon and Jacques Babinet in 1843 [26].

A fiber is consists of three layers: core, cladding and jacket. Core is the inner part with high refractive index, cladding is the middle part with a lower refractive index, and jacket is the outer protective polymer layer (PVC, plastic etc.) [27]. Figure 18 shows the layers of optical fibers.

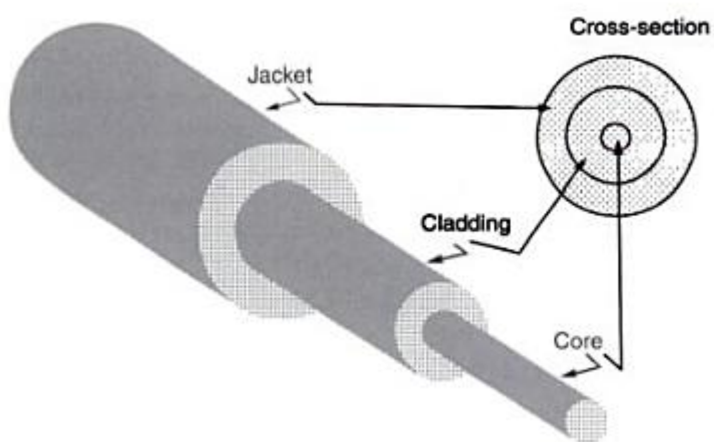

Figure 18: The schematic view and cross section of an optical fiber [27].

Fibers have a certain numerical aperture (NA), defined as the sinus of the largest angle an incident ray with respect to the fiber axis. The range of angles, at which the fiber accepts or emits, changes up to the numerical aperture.

For instance, a numerical aperture of 0.22 corresponds to 12.7° approximately. In this case, the emitting light leaves in a cone that is ±12.7°. The numerical aperture of a fiber is calculated as in Equation (3.1) [28].

$$NA = \sin(\theta_m) \tag{3.1}$$

where NA is the theoretical numerical aperture and θ_m is the largest incident of ray angle that the fiber guided. The numerical aperture can also be calculated in terms of index profile as in Equation (3.2).

$$NA = \sqrt{n_1^2 - n_2^2} \tag{3.2}$$

where n_1 and n_2 are the maximum refractive index of core and cladding, respectively. The refractive index between cladding and core limit the NA.

However, a near to eye display design requires the light to scatter a short distance. Due to the distance limitation of the present design, how to make numerical aperture expansion becomes an important question.

The fiber used in this thesis is a glass clad multimode optical fiber, 0.22 NA silica core with 50 um core and 125 um cladding diameter.

For a NED design, the space on which the light has to expand is too short. It is not possible for light to scatter such a short distance with conventional methods. So a point source containing scattering particles is fabricated.

When we look at clouds or sky, what we see is scattered sunlight. The reason why we see a leaf as green is that it scatters green light more than it scatters red light [29]. Light scattering is a form of scattering in which light is scattered in the form of propagating energy. Scattering is the redirection of electromagnetic waves due to their interaction with matter. The intensity and direction of the light change according to the wavelength of the light and particle properties such as shape and size [30].

Light scattering models are divided into three models according to the comparison between particle size and wavelength of the incident light. Mie scattering occurs when the particles are approximately equal in size to the wavelength. Geometric Mie scattering occurs when particles are much larger than the wavelength. In this case, geometric optics such as reflection and refraction is used to explain how light scatters [30]. Rayleigh scattering predominates if the particle size is smaller (<1/10) than the wavelength of the incident light [31, 32].

Figure 19 shows Mie scattering and Rayleigh scattering patterns. The Rayleigh scatter is mirrored in the forward and backward directions contrary to Mie scattering.

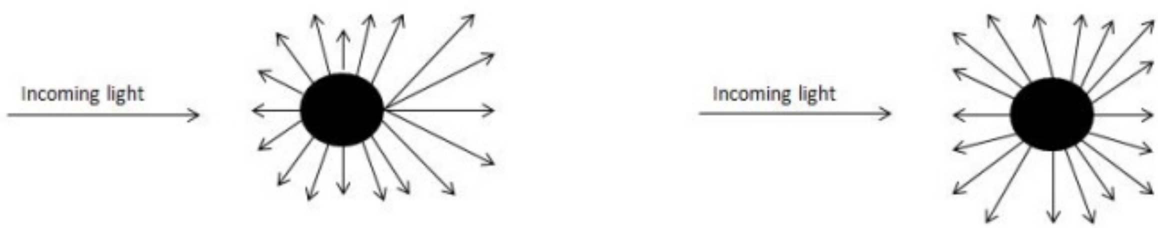

Figure 19: Scattering Types a) Mie Scattering b) Rayleigh Scattering.

The particle size of particulate Zinc oxide (ZnO) and Titanium dioxide (TiO_2) have scattering nanoparticles that are used in UV protection inherent in sunscreens and cosmetics [37, 38]. The refractive index of ZnO is 2.0041 whereas the refractive index of TiO_2 is 2.6142. As the ozone layer in the Earth's atmosphere becomes thinner, protection from harmful UV light becomes an increasingly important matter. Therefore, the reason to use ZnO and TiO_2 nanoparticles in UV protection is the efficiency of small particles at scattering shorter light wavelengths [38].

3.2.2. Creation of the point light source – scattering, particle size

In this thesis, scattering nanoparticles are used to extend the angle at which the fiber emits light. The point source should scatter in every direction with equal likelihood.

Since we performed our experiments with red light, the particle size of the scattering particle should be under 65 nm. TiO_2 transparent nano powder whose hydrodynamic particle size is 21nm is used in the experiments as TiO_2 rather than ZnO is the higher refractive index of TiO_2.

The PLS is fabricated as follows: 1) A mixture of 1 ml epoxy and 0.2 gram TiO_2 powder is prepared and the fiber is dipped into this mixture. 2) The jacket of the fiber is removed using a stripper to ensure that nanoparticles are present only at the tip of the fiber. In this way, unintended scattering over an extended length of the fiber tip is prevented 3) Nanoparticle-epoxy mixture at the tip of the fiber is cured by exposure to ultraviolet light. Figure 20 shows microscopic images of the fiber before and after dipping into the nanoparticle-epoxy solution and stripping.

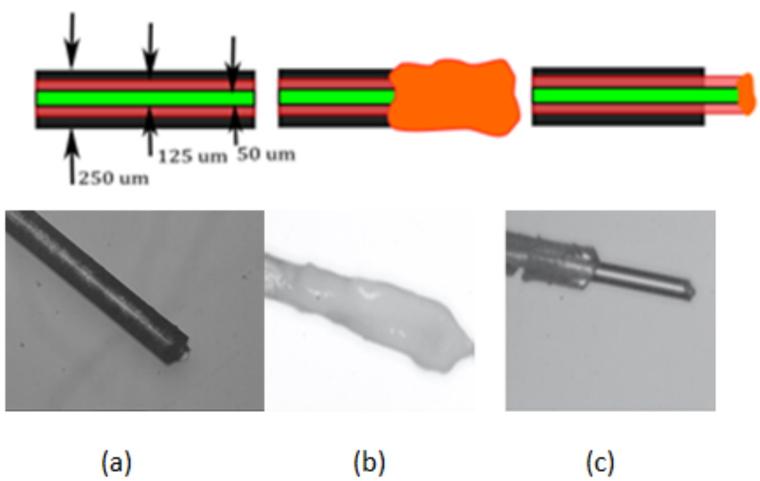

Figure 20: Fiber with the PLS at the tip – fabrication steps (top row) and microscope images (bottom row). (a) the fiber, with the core (green), cladding (red), jacket (black) (b) the fiber dipped into nano particle-epoxy mixture (c) the fiber stripped of the jacket, with the nano particles remaining only at the tip.

An experiment was conducted to verify that the fabricated structure indeed acts as an isotropic PLS (Figure 21a). A diffusive hemispherical screen was obtained by cutting half of a table tennis ball. A camera was placed on the side.

When the fiber tip was placed at the center of the hemisphere prior to the fabrication steps, only a small spot formed on the screen. After the addition of the nanoparticles though, we obtained the image in Figure 21b. As expected, the hemisphere is illuminated almost completely and uniformly.

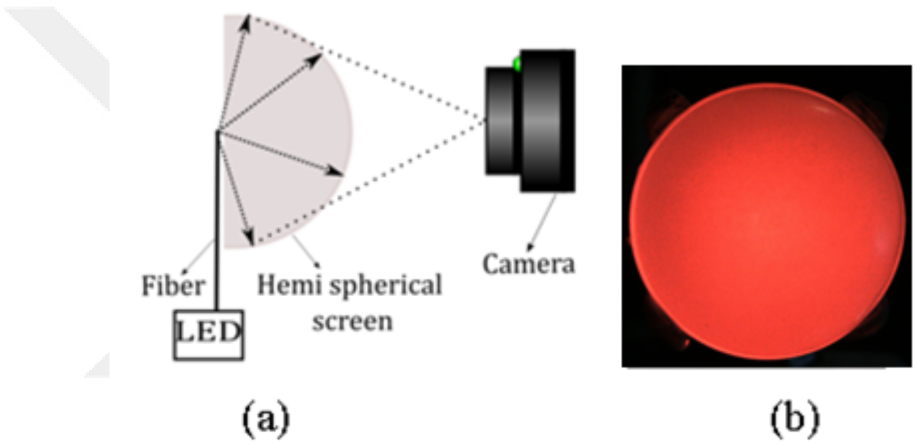

Figure 21: Experimental verification of the fabricated structure. (a) Experimental setup. (b) Captured image of the hemispherical screen verifying that fabricated structure acts as an isotropic PLS.

Three experimental prototypes are presented to verify our design. The first one is a proof-of-concept non-compact design that uses an off-the-shelf large radius spherical concave mirror. The second prototype is a compact design in which we manufacture a low f-number concave mirror by covering the curved surface of an off the shelf plane convex lens with a semi-transparent chromium layer. The third prototype uses an ellipsoidal mirror we designed and was fabricated by a company via diamond turning.

Figure 22 illustrates the generic design for the generation of a converging wave for all these prototypes. Light from an LED or laser source is coupled to a multi-mode fiber. Minute amounts of nanoparticles deposited at the tip of the fiber scatter the exiting light and create a high NA PLS. The PLS is positioned on the optical axis. The light rays, upon getting reflected by the curved surface, are converted into a converging wave. On the converging wave path, a transmissive LCD or an SLM can be placed to realize a pinhole or a holographic NED, respectively. The position of the PLS can be adjusted to change the degree of convergence and hence the FOV supportable by the CBI.

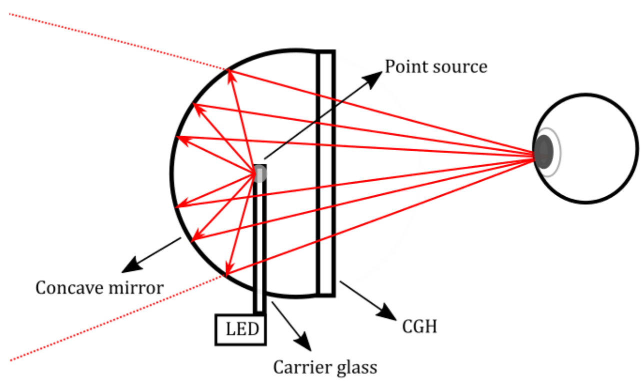

Figure 22: Generic design of the coherent backlight illuminator (CBI). LED or laser light is coupled to a multi-mode fiber inserted in a transparent carrier rod. Nanoparticles are placed at the tip of the fiber to expand NA and create an isotropic PLS. A small blocker spot placed on the right of the fiber tip confines the emitted rays to the left hemisphere. Emitted rays are reflected from the concave mirror and form a coherent converging wave, on the path of which a transmissive LCD or an SLM can be placed to realize a pinhole or holographic near-to-eye display (NED).

3.2.3. Bulky Configuration

Once the fiber based PLS is ready, we conducted our first experiment. Here, we did not pursue a compact design. Rather, we wanted to make sure that the reflector has a high optical surface quality. In this way, we could attribute any reduction on the generated beam quality, if any, solely to the fabricated PLS. With this perspective, we used an off the shelf spherical concave mirror with f=56.25 mm and 75mm diameter as the reflector. We placed the PLS at a distance of 80 mm from the mirror vertex and obtained a wave converging at a distance of 186 mm. The obtained converging wave supports a FOV of 70 degrees. To demonstrate a holographic NED, we computed a binary CGH, which was printed as a chrome on glass mask. The CGH mask has a pixel pitch of 2um and is designed to form an eye box of 2 mm when illuminated with a wave (at a wavelength of 632 nm) converging at a focus point 20 mm away. As the light source, we first used a 660 nm LED. The image delivered by the system is shown in Figure 23.

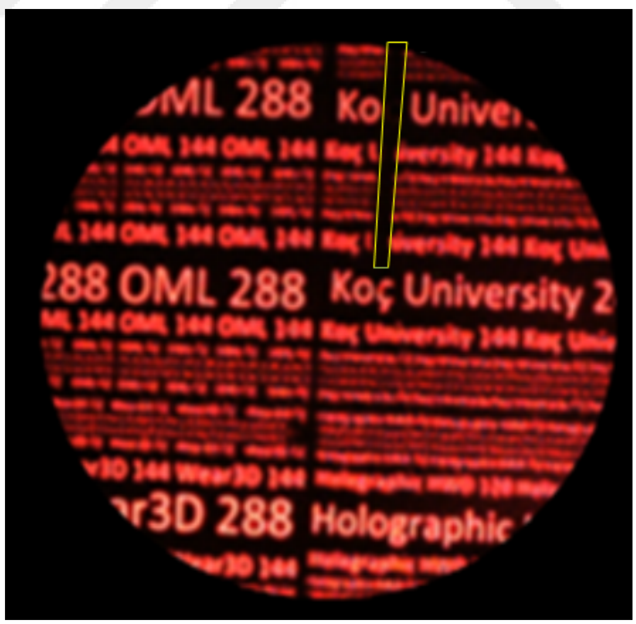

Figure 23: The image seen from the CGH mask using LED.

First, we put the fiber with the PLS at the tip inside a syringe needle, which is why there is a shadow in a shape of black line in Figure 23 (Shown inside the yellow borders). In order to prevent this shadow, the next step is to embed it into a rigid carrier rod so that the position of the PLS in the CBI is precisely controlled. So as not to disturb the viewer, the rod should be transparent, and visually non-recognizable. In our experiments, we implemented the rod by sandwiching the fiber between a piece of plexiglass and an epoxy layer. A number of chemical processes are performed to ensure that the epoxy layer is flat, thin and index-matched: 1) We prepare a mixture of aquaphobe and hexane (10% v/v solution in hexane) 2) We dry a microscopic glass slide on a hotplate for several minutes at 100°C after which we put the slide into the aquaphobe solution and wait for around a minute. 3) We take the glass slide out of the solution and wipe it by blowing the excess dry using N_2. 4) We put the dry glass slide on the hot plate at 60°C and wait for 4 minutes. Afterwards, we rinse the slide with hexane and then with acetone. 5) We put our fiber between the dried and rinsed glass slide and a sheet of plexiglass, and then inject optical adhesive epoxy in between. The capillary force causes the epoxy to be distributed between the plexiglass and slide. 6) The epoxy is UV cured for 5 minutes, after which the glass slide is removed. Figure 24 shows the steps of fabrication. Figure 25 shows the experimental setup after embedding the fiber with PLS into a transparent, indexed match carrier rod and Figure 27a shows the image delivered with transparent carrier rod.

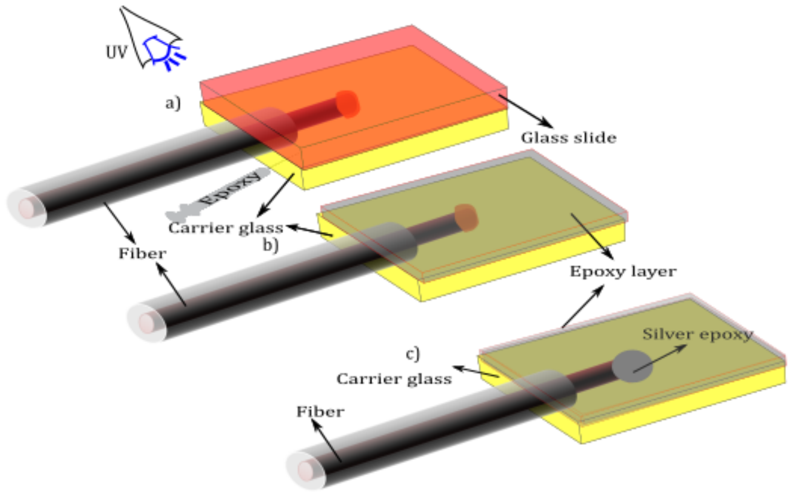

Figure 24: Embedding the fiber with PLS into a transparent, indexed match carrier rod. (a) Fiber is placed between a layer of plexiglass (yellow) and an aquaphobed glass slide (red) and epoxy is injected in between. b) After UV cure, glass slide is removed. C) Silver epoxy is placed as blocker spot.

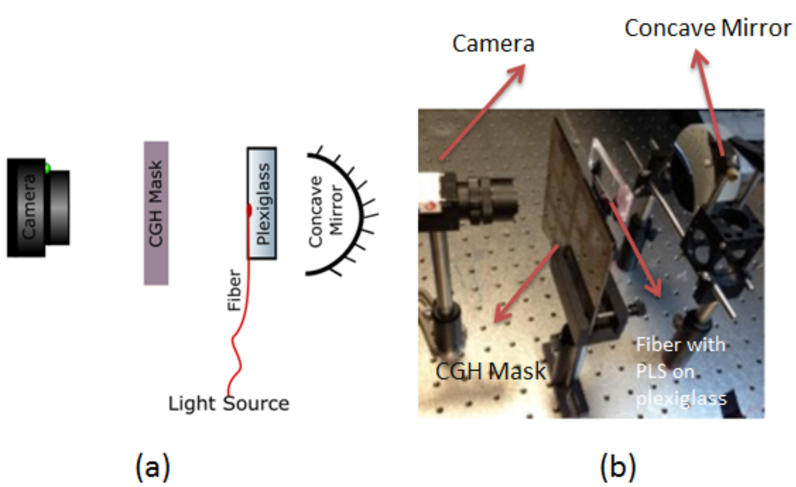

Figure 25: Experimental setup after embedding the fiber with PLS into a transparent, indexed match carrier rod a) Illustration b) Realized prototype.

3.2.3.1. Direct light problem, silver epoxy solution

In Figure 27a, a bright spot is present in the middle because we have not yet blocked the light coming directly from the PLS without getting reflected by the concave mirror.

We did not see this bright spot in Figure 23, because the tip of the syringe needle has a special beveled shape as in Figure 26. The longer part of the needle is positioned to the eye; hence, we managed to block the direct light.

Figure 26: Shape of the tip of the needle.

To block that direct light in our PLS design with a transparent rod, we place a small piece of silver epoxy on the viewer side of the carrier rod, as in Figure 24c. Figure 27 shows images obtained before and after the placement of the silver paint. The Figure 27b shows that the direct light is blocked without causing any noticeable degradation in image quality.

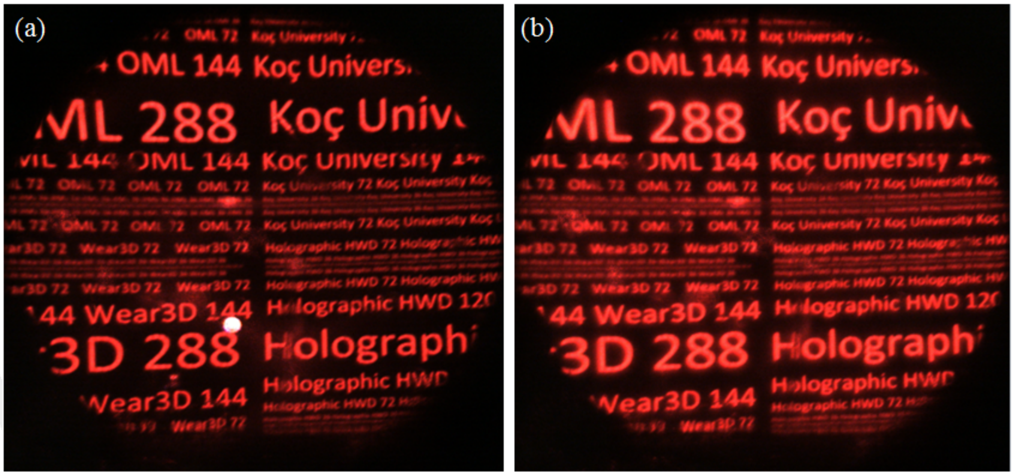

Figure 27: Correction of the bright spot problem (a) with bright spot (b) without bright spot.

3.2.3.2. Laser vs LED Comparison

In addition to the LED source, we conducted the experiment with a 632 nm He-Ne laser source. Figure 28 shows the obtained images in a comparative manner. As expected, the image with the laser has better resolution but is corrupted with speckle noise. Although the CGH mask is designed not be affected by speckle, the 125 um source creates this speckle problem. Speckle is washed out with the LED source and an image with much uniform brightness emerges, though at the cost of loss of resolution.

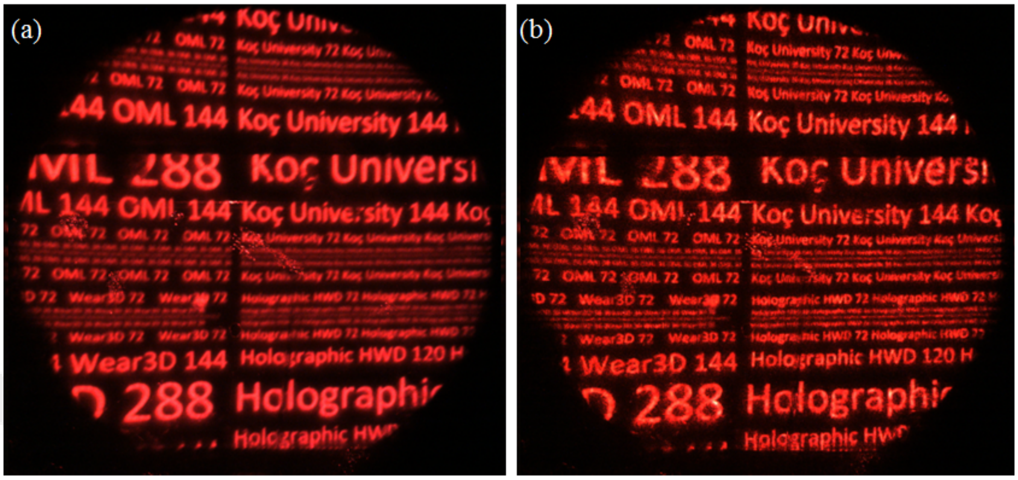

Figure 28: Captured images with a) LED, b) Laser.

3.2.4. Second experiment with the coated plano-convex lens

In the second experiment, we pursued a compact design. Since an off-the-shelf concave mirror with a short focal length (30-40 mm) and low f-number is not available, we decided to manufacture our own mirror. In this respect, we covered the curved side of an off the shelf short focal length plano-convex lens (Thorlabs LA1274, R=20.6 mm) with chromium via sputtering. The layer thickness is adjusted to 10 nm in order to obtain a semi-transparent CBI.

The difficulty while sputtering the lens is to cover it with metal without any scratches. The sample must be screwed to fix the sample in sputter. However, screwing the edges of the lens may harm it so we used AZ9260 Photoresist to paste the lens on top of a microscopic slide. After soft baking the slide and the lens at 100°C for 1 minute, we pasted them to each other using the photoresist and performed post baking at 100°C for 25 minutes. After covering the glued lens, we cleaned it from photoresist using acetone and IPA. Figure 29 shows how we fix the glued lens on the sputtering target with screws.

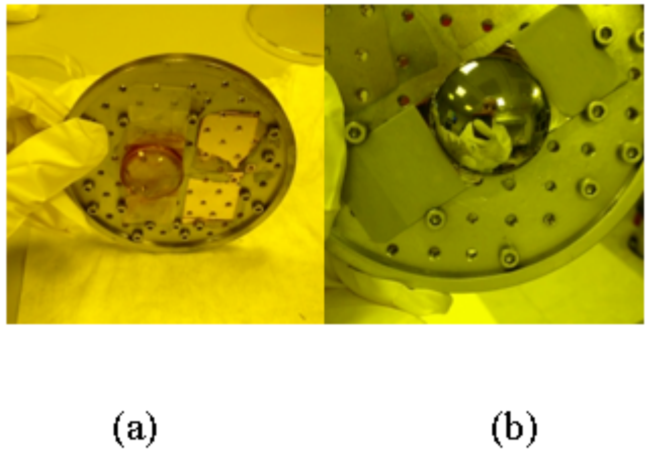

Figure 29: a)Lens is attached on top of a microscopic slide using photoresist. b) The edges of microscopic slide is screwed on sputtering target to prevent scratches that may be occur on the lens.

As a result, rays from the PLS undergo a refraction on the planar lens side, then a reflection at the curved side, and then another refraction on the planar side. Zemax simulations are conducted to determine the new focus positions. Afterwards, the CGH used in the first experiment is placed in the converging beam path, and the image shown in Figure 30 is obtained.

The most challenging part of the proposed design is to fix the fiber with PLS in the correct position. First we stapled the fiber with PLS with the help of a syringe needle. In Figure 30, the shadow of the needle is seen in the middle of the captured image. As a next step, we embedded the fiber with PLS into a transparent, indexed match carrier rod as explained in Figure 24. Figure 31 shows experimental setup, Figure 32 shows the result and Figure 33 shows the realized prototype.

Figure 30: Image captured when fiber is fixed with a syringe needle.

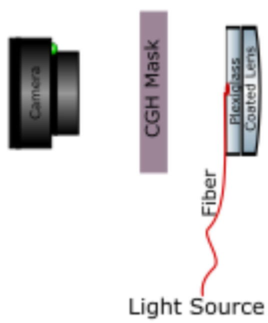

Figure 31: The experimental setup for compact design.

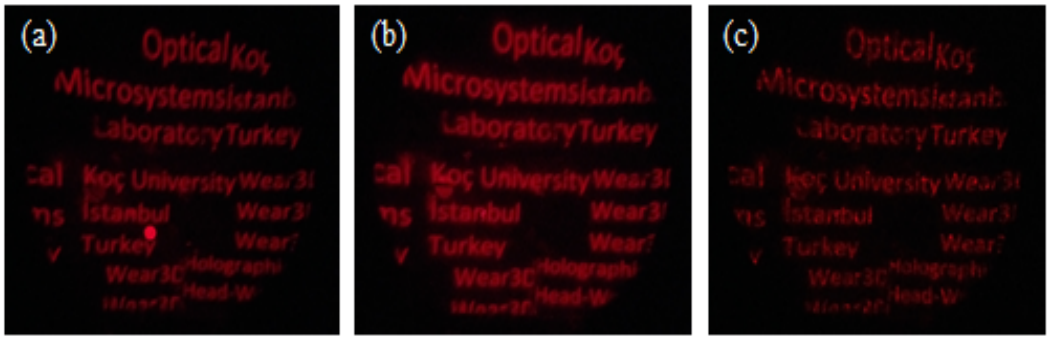

Figure 32: Images captured after the embedment process a) With bright spot problem when LED is used b)Without bright spot when LED is used c)When laser is used.

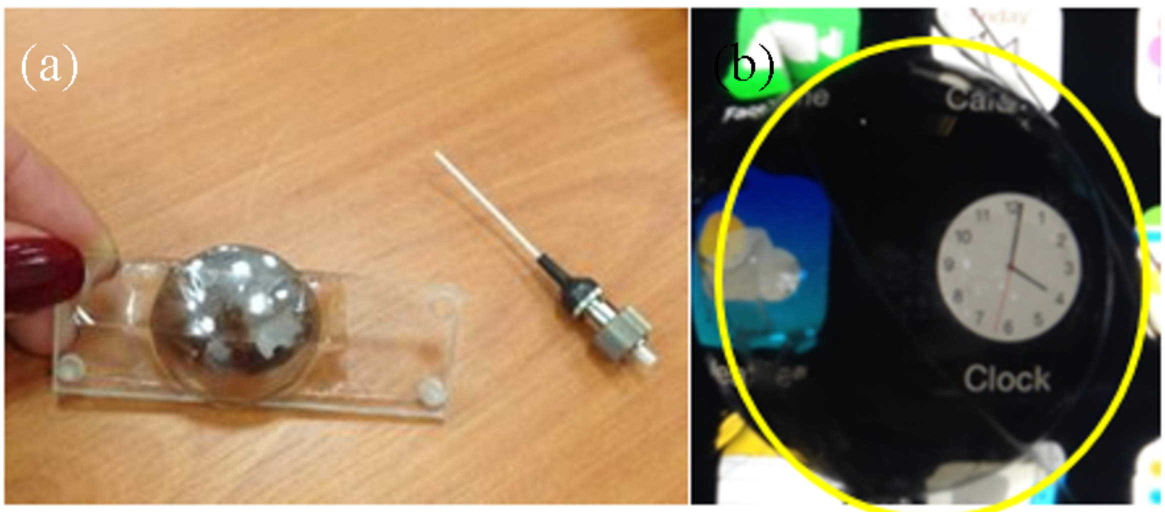

Figure 33: a) The tip of the fiber is stuck on a plexiglass with 3mm thickness is and fixed at the center of the concave mirror. b) A transparently thin coating of metal on glass allows reflections from both the glass and backside.

The effective focal length of the metal coated plano-convex lens is affected by the following interactions: 1) Refraction through the first surface, 2) reflection through reflective surface, 3) refraction through first surface again.

In order to find the exact focal point, we performed simulations on ZEMAX. Figure 34 shows the simulation layout. The thickness of the plexiglass is 3 mm, and the thickness of CGH is 2.4 mm.

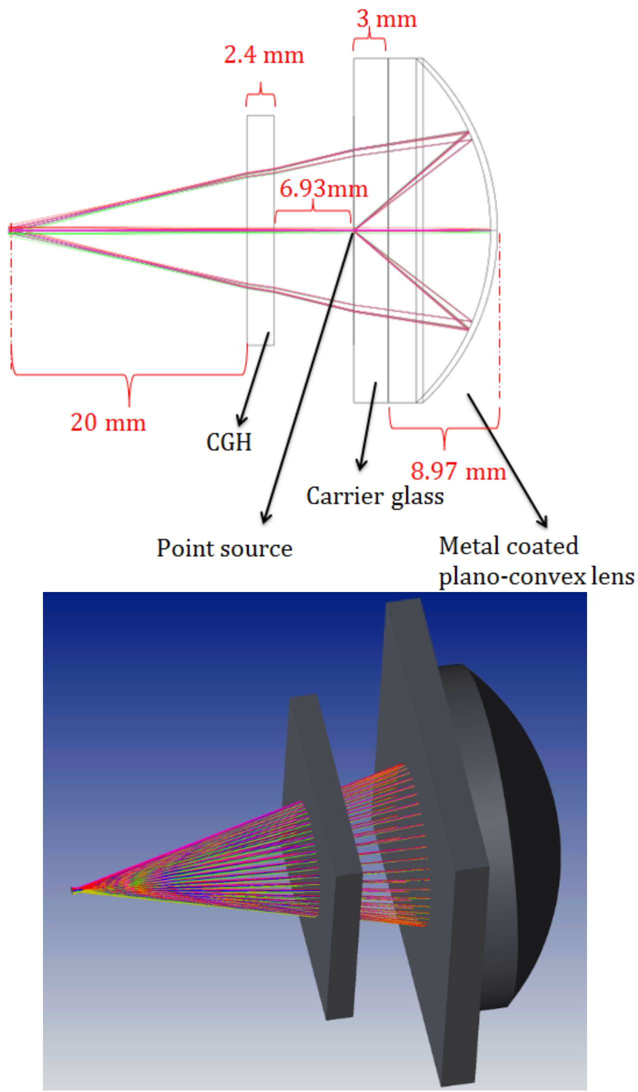

Figure 34: ZEMAX simulation showing the layout of the rays out of the point source.

3.2.5. Third Experiment with Ellipsoidal Mirror

The CBI designed and used in the second experiment is compact and provides a wide FOV. However, the spherical nature of the reflector, as well as the presence of the lens material between PLS and reflector leads to severe spherical aberrations in the generated converging wave. To remedy that problem, we conducted a third experiment. This time, we designed an ellipsoidal reflector such that we place the PLS at one focal point and obtain the focus spot of the converging wave at the other focal point. Our intention has been to make use of the fact that an ellipsoid performs perfect imaging between its two foci, so that we can in principle completely avoid aberrations.

Ellipsoidal mirrors have a special property. They have two focus points. These two focus points (foci) lie on the major axis of the ellipse. A light ray leaving from one of these focus points always passes through the other one. In other words, light rays originating from the first focus point converges on the second focal point.

The advantage of using an ellipsoidal mirror is to avoid spherical aberration that we encountered in the spherical mirror case.

Ellipses have two perpendicular axes. The longer one is called *major axis* and the smaller one is called *minor axis*. One half of these axes are called *semi minor* and *semi major axes*. The two foci of the ellipse are equidistant. In Figure 35 a and b show semi major and semi minor axis; points labeled as f are the foci.

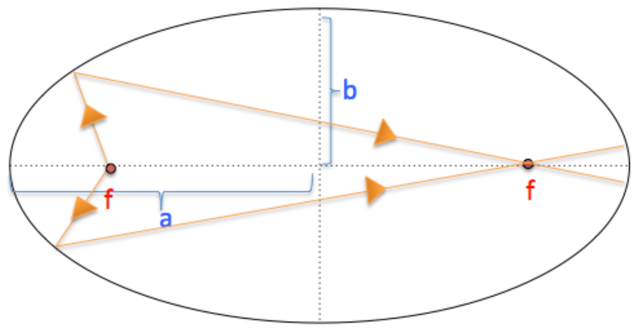

Figure 35: Ellipsoidal mirror concept

General equation of an ellipse is written in Equation (3.3)

$$\frac{x^2}{a^2}+\frac{y^2}{b^2}=1 \tag{3.3}$$

where a and y are the coordinates of any point on the ellipse and a and b are semi axes lengths.

The coordinates of focuses are found with the following equation

$$f=\sqrt{a^2-b^2} \tag{3.4}$$

Placing the point source at the first focus point will result in the light rays converging on the second focus point. We calculate the coordinates of these points using the equation above. Since the binary CGH mask must be placed in front of the converging point with a certain distance d, coordinates of the mask can be calculated easily. Figure 36 shows the sketch of the locations of CGH mask and point source.

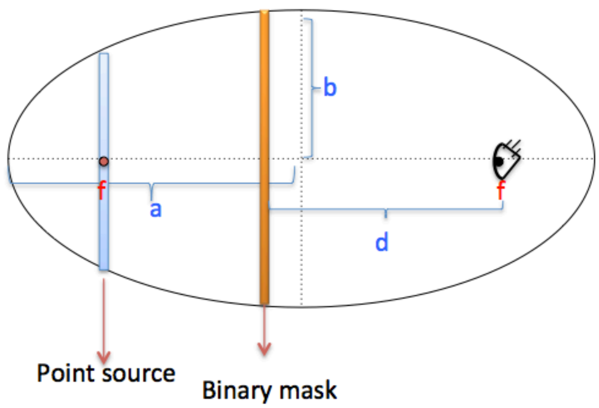

Figure 36: Locations of point source and the binary mask on the ellipsoidal mirror design.

The diagonal FOV is calculated for a 20mm x 20 mm CGH mask. Assuming light rays are coming from point C in Figure 37, the CGH mask is illuminated with 2a angle.
The calculation is made using the Pythagorean theorem. Figure 37 shows the ABC rectangle on which we used the theorem where d denotes the distance between the CGH mask and the light source.

$$\alpha = \arctan\frac{10\sqrt{2}}{20} = 35.26°$$

$$2\alpha = 70.52°$$

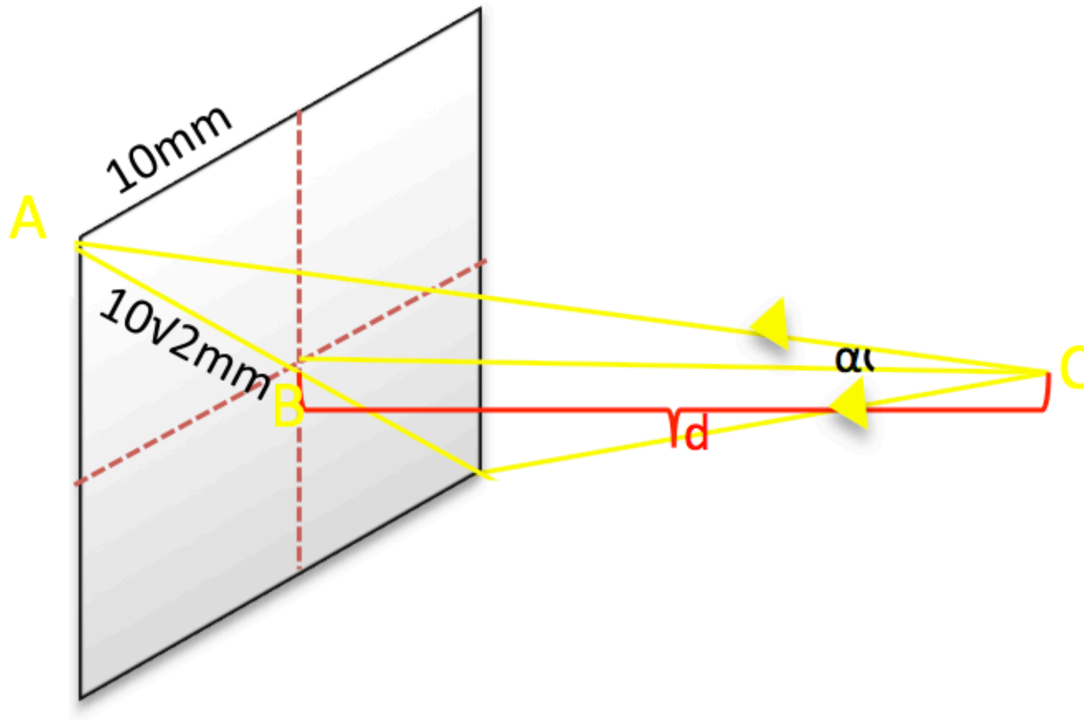

Figure 37: Diagonal FOV calculation for 20mm x 20 mm binary CGH mask.

Since we have a 20 mm x 20 mm binary CGH mask, we calculated the FOV according to those measures. However, with a bigger CGH mask it is possible to get higher FOV values. We want to make a compact design, so we want to put the point source and the binary CGH mask into the half of an ellipsoid whose inside is covered with metal, so that it becomes an ellipsoidal mirror with two foci.

For different semi major axis and semi minor axis lengths, the coordinates of the foci change as well as the dimensions of the CGH mask that can fit into the semi-ellipsoid.

In order to make such a compact design, we need to know the dimensions of the transparent carrier on which we will put the fiber with nano-particles. Since the point source will be placed on the focus point that is inside the semi-ellipsoid, it is easy to calculate the dimensions of the transparent carrier. The distance from one of the focus points of an ellipse to itself, measured along a line perpendicular to the major axis is called semi-latus. Semi-latus length l is calculated as in Equation (3.5)

$$l = \frac{b^2}{a} \tag{3.5}$$

For Zemax simulations the ellipse is modeled with the standard surface. Semi major and semiminor axis lengths of the ellipsoidal surface is converted to radius and conic descriptions.

Vertex radius r is calculated using Equation (3.6) and conic constant k is calculated using Equation (3.7) where a and b are semi major and semi minor axis lengths respectively. Conic constant for ellipse is always between -1 and 0.

$$r = \pm\frac{b^2}{a} \tag{3.6}$$

$$k = \frac{(b^2 - a^2)}{a^2} \tag{3.7}$$

For an ellipsoidal mirror with a=25mm and b=21mm we specified three different fields in the field data dialog window. The reason for specifying different fields is to take the possibility for the point source to shift into consideration.

ZEMAX plots the spot diagram for each field point. The shift of the point source causes a shift in the IMA (image location) in spot diagrams. The first defined field in simulations is without any shift, the second and third fields include 0.1 mm and 0.2 mm shift on the y axis.

For this geometry, the focus is calculated as f=13,5647 mm. When we put the point source 13,5647 mm away from the center of the ellipsoid, we expected the light to converge 13,5647mm away from the center of the ellipsoid in the reverse direction. With our first simulation, we crosschecked coordinates of the focus points and the ellipsoidal geometry we designed in ZEMAX. Figure 38 shows the converging light rays coming out of calculated focus point. Figure 39 shows the spot diagram for three different fields. RMS and geometrical radii increased as the shift increase. Whereas there is no shift, the RMS radius is 6.873 um, however with 0.1 mm shift of point source RMS radius becomes 185.275 um and with 0.2 mm shift it is 370.355 um. It is also obvious that a shift in y axis creates coma aberration.

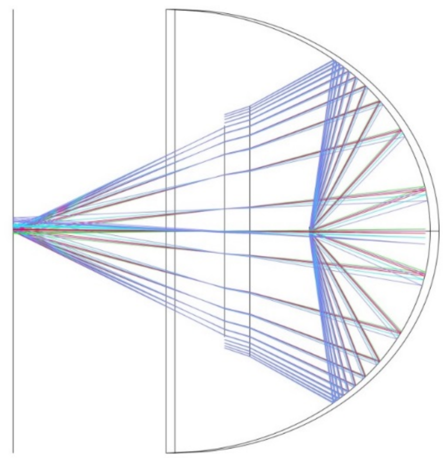

Figure 38: Zemax Simulation showing how incoming light converges.

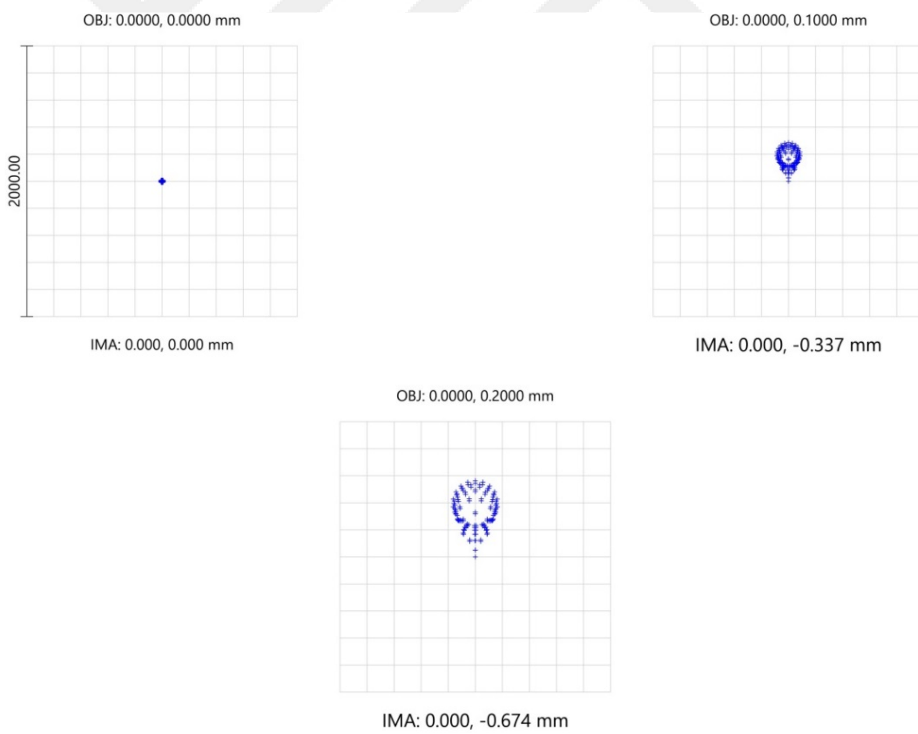

Figure 39: Spot diagram for three different fields.

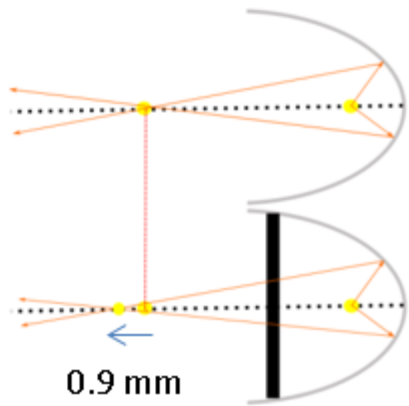

Figure 40: Focus shift due the thickness of the CGH mask.

3.2.5.1.Ellipsoidal Mirror Fabrication

3.2.5.1.1.First Trial: 3D Printing

After deciding the dimensions of the ellipsoidal mirror, first we drew the semi-ellipsoid in the 3D modelling program Solidworks. Later we printed it via 3D printer. The plastic filament 3D used was white Acrylonitrile butadiene styrene (ABS). The printer is UP Plus 2 (150 micron detail).

ABS is a thermoplastic that is used in Lego and bumpers in automobiles thanks to its strength, toughness, temperature resistance and durability [39]. ABS is based on three monomers that it contains: Acrylonitrile, Butadiene and Styrene.

In order to decrease the roughness level of the 3D object, we used Methyl ethyl ketone (MEK), also known as Butanone. We rinsed the 3D ABS part with MEK and hence got a smoother surface.

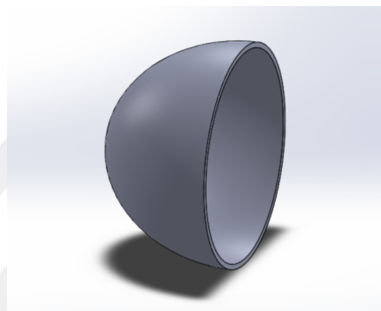

Figure 41: 3D model of ellipsoidal mirror.

Figure 42: Chromium covered 3D printed semi- ellipsoids.

After preparing 3D semi-ellipsoid parts we plated them with chromium via galvanization. Figure 42 shows chromium plating on ABS plastic. As can be seen from this figure, plating was not bright enough and chromium does not cover the inner surface of the semi-ellipsoid. Hence we decided on changing the production method to produce the semi-ellipsoids.

3.2.5.1.2.Second Trial: Injection Molding

Injection molding is a popular way to produce plastic parts. Molten plastic is injected into a mold which is in the form of the part to be made. The mold is prepared in CNC.

Plastics are divided into two: Thermoplastics and thermosets. Thermoplastics have the property to solidify after heating, being softened, and melted. However, thermosets are degraded by heat [40]. Because of this reason, thermoplastics are primarily preferred for injection molding applications.

Figure 43 explains the injection molding process briefly. 1) Granules of plastic powder are put into the hopper. 2) The tube is heated and when it reaches high temperature, a screw thread starts turning. 3) The thread is turned by a motor, the plastic granules go along the heater part, so they became liquid. The liquid goes to the mold part and it cools inside the mold.4) The mold is open and the plastic object is removed.

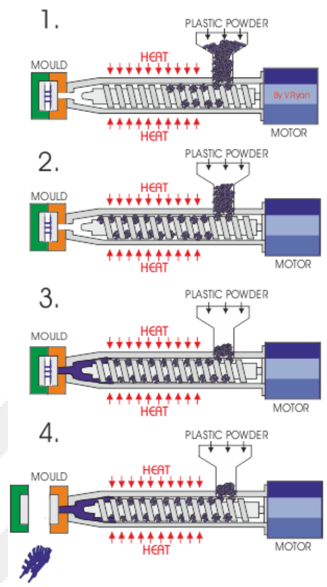

Figure 43: Injection Molding Process [42].

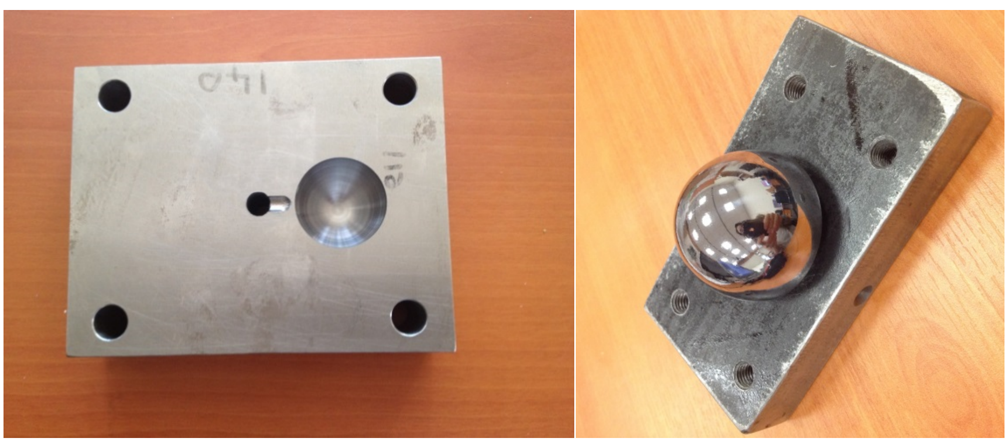

Figure 44: Molds fabricated via CNC.

Figure 45: Injection molding machine.

Figure 44 shows molds fabricated via CNC, Figure 45 shows the injection molding machine, Figure 46 shows the CNC machine used, Figure 47 shows the ABS powder used. ABS powders are first put into an oven to dehumidify.

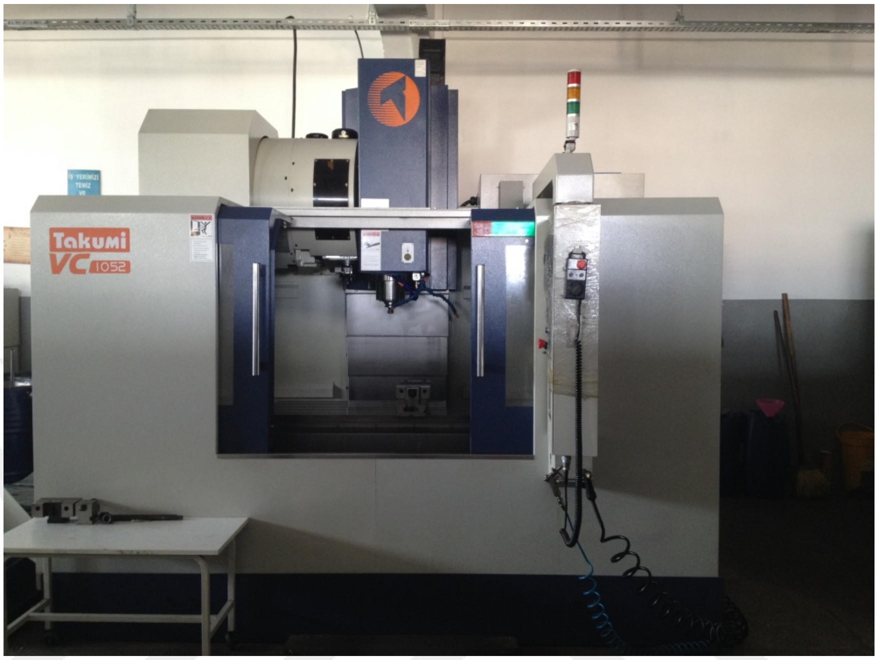

Figure 46: CNC machine used to fabricate

Figure 47: ABS powder that is melted in the injection molding machine

.

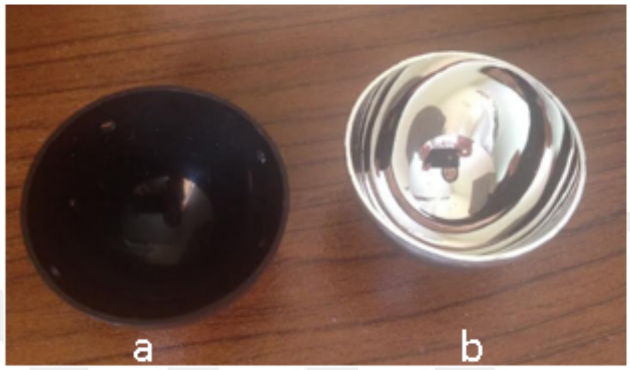

Figure 48: Semi ellipsoidal plastic parts a) Before covering with metal b) After covering with metal.

Atomic force microscopy (AFM) is used to measure the roughness of chromium plated CNC produced part. The measurements are done with Bruker Dimension Icon with ScanAsyst mode in air. The model of the cantilever is SCANASYST-AIR, k=0.4 N/m, frequency 70kHz. Five different images are captured with the same tip from different parts of the sample. Figure 49 shows the captured images. NanoScope Analysis 1.5 program is used to make roughness calculations and to export the images. Using the bar on the right side of the images, it is possible to comment on the dimensions of the biggest cracks. Table 1 shows Rq and Ra values of these 5 images. Rq average of these 5 images is 21.8 nm Ra average is 16.9 nm.

There are many different roughness parameters. R_a and R_q are the most common ones. Equation (3.8) and (3.9) shows how R_a and R_q are calculated [41].

R_a gives a description of the height variations in the surface, it is also called *mean roughness*. R_q is also called *RMS roughness.*

$$R_a = \frac{1}{N}\sum_{j=1}^{N}\left|Z_j\right| \tag{3.8}$$

$$R_q = \sqrt{\frac{\sum Z_i^2}{N}} \tag{3.9}$$

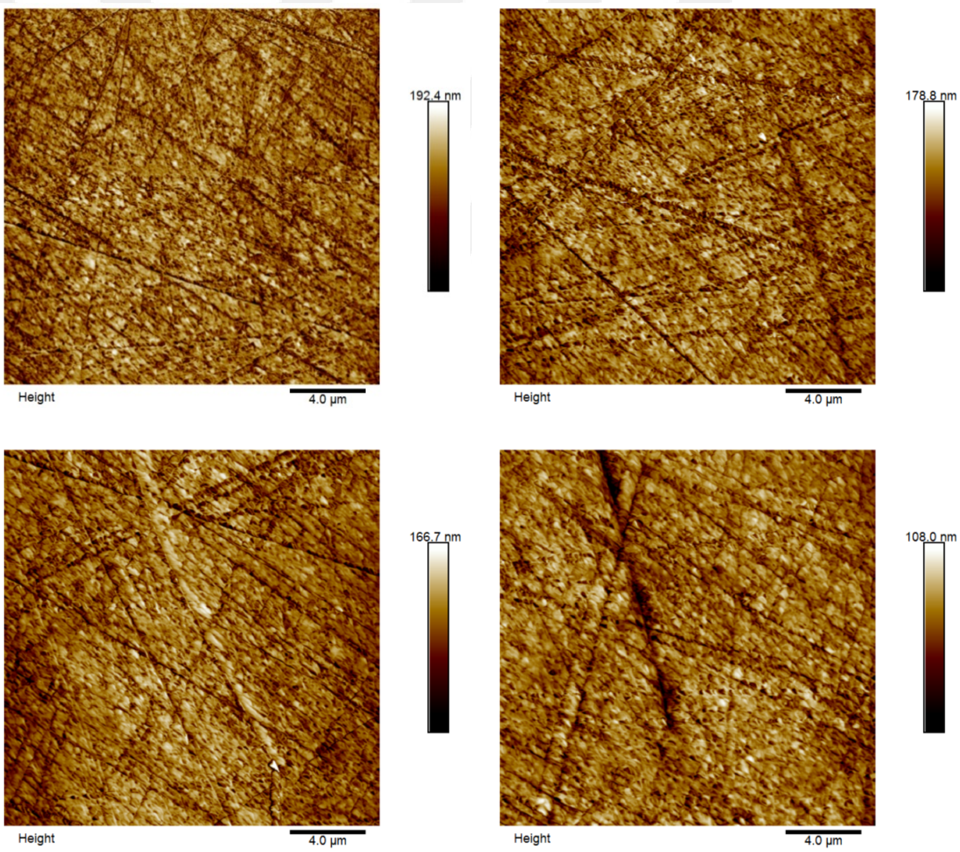

Figure 49: Captured images from the surface of the CNC produces chromium plated sample via Bruker Dimension Icon with ScanAsyst mode in air Image size 20 um.

Table 1: Measurement results of AFM.

Image number	Image Rq (nm)	Image Ra (nm)
1	27,3	21,4
2	25,4	20
3	18,6	14,4
4	23,2	18,1
5	14,5	10,9

The experiments performed with the semi ellipsoidal mirrors fabricated with injection molding technique gave good RMS roughness but it did not give proper results for our application because the form of the ellipsoid is deformed. So we changed the production method.

3.3.5.1.3. Third Trial: Custom Mirror Production via Diamond Turning

An ellipsoidal mirror is manufactured via diamond turning process by Diffractive Optics Ltd. in Hong Kong. The mirror is on Nickel substrate and covered with aluminum coating. The precision is below ʎ/20 across any 3 mm diameter area which corresponds to a 10nm Ra.

Diamond Turning is a multi-stage process. At the initial stage, metal shaping is performed via CNC; later, to increase accuracy, a diamond-tipped lathe tip is used.

This technique is commonly used in manufacturing optical elements from crystals, metals, acrylic and other materials. These optical elements are widely used in telescopes, video projectors and scientific research instruments. One of the main advantages of the diamond turning techniques is that it does not require any additional polishing or buffing as other conventional machine surface techniques do. Figures 50 and 51 illustrate the manufactured mirror with dimensions with tolerances.

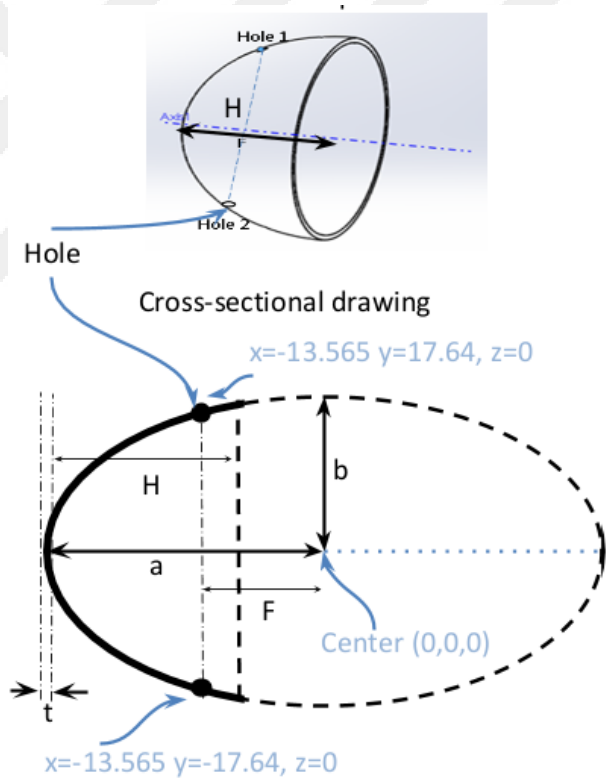

Figure 50: Dimensions of the manufactured mirror

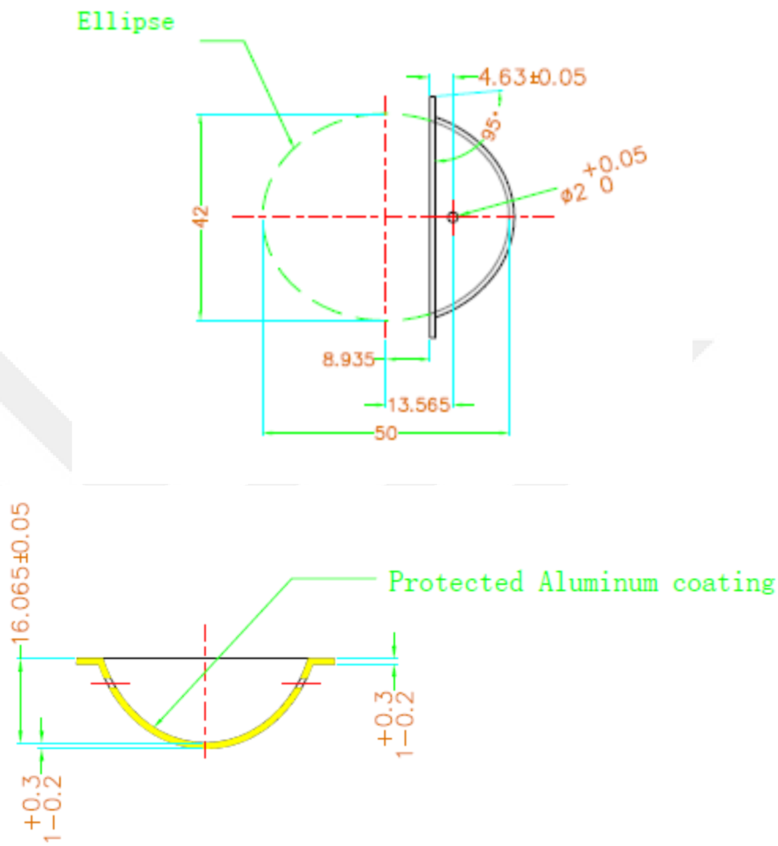

Figure 51: Dimensions of the manufactured mirror

A 3D printed module is used to fix the mirror, fiber and the CGH mask. Drawing of this module is shown in Figure 52a, and the realized prototype is shown in Figure 52b.

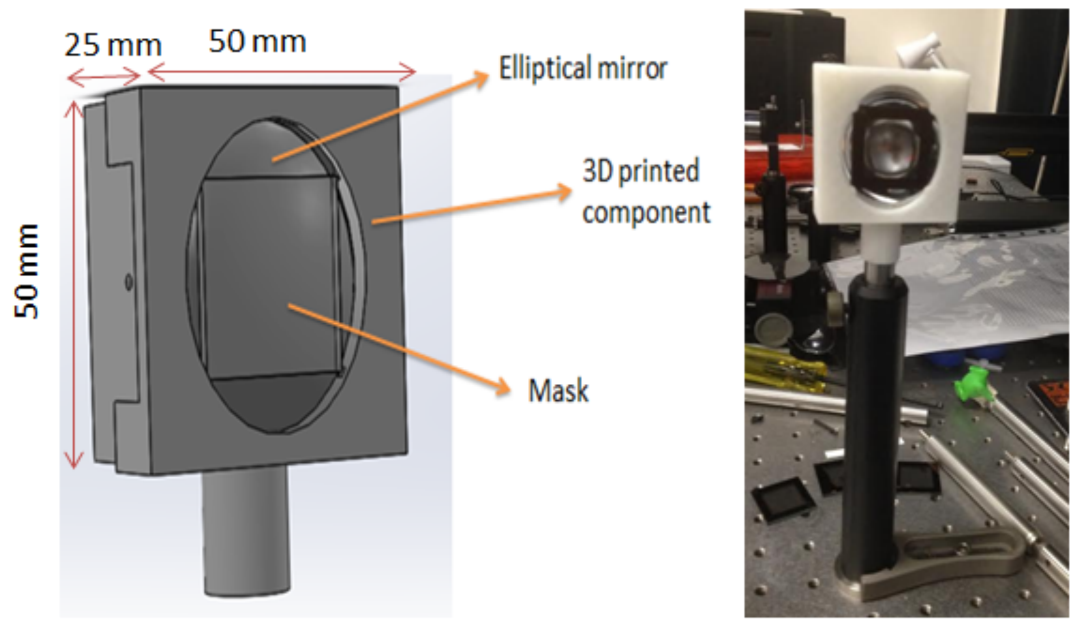

Figure 52: a) Drawing of 3D printed module b) Realized prototype

In order to fix the fiber in the 3D module, 2 different approaches are attempted. First, the fiber is fixed on top of a carrier glass (acetate paper). Figure 53 shows the image captured with this approach.

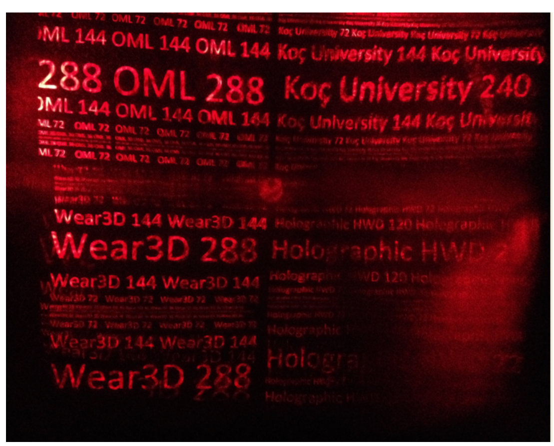

Figure 53: Image captured with ellipsoidal mirror while fiber is fixed on an acetate paper.

Since acetate paper is too elastic but the holes in the ellipsoidal mirror are not big enough to fix a thick plexiglass inside, a syringe needle is used to fix it. This time the letters on the CGH mask become clearer. Figure 54 shows the image captured with a syringe needle. Although the needle blocks some part of the letters, it is easy to read the letters on the left part of the image.

Figure 54: Image captured with ellipsoidal mirror while fiber is fixed with a syringe needle.

4. CONCLUSION

In this thesis, a novel design to construct a backlight illuminator for near to eye displays capable of presenting wide FOV is demonstrated. The proposed design combines a fiber, scattering nanoparticles and a concave mirror/ellipsoidal mirror. Point source fabrication and different designs for point source usage is presented.

Near to eye displays should be small and compact. With conventional methods it is not possible for light that emitted out of fiber to scatter in such a short distance. Nanoparticles used in sun creams are used to scatter light in short distances. After preparing PLS, CBI is tested with an off-the-shelf concave mirror. This was a bulky design. A smaller concave mirror is required for practical use. A semi-transparent and smaller concave mirror is fabricated via plating a plano convex lens. Since the metal thickness was too thin (10nm), this plano convex lens becomes a transparent mirror. The problem with this design is that this mirror also acts as a magnifier glass. In order to prevent this magnification, top of the covered lens may be covered with epoxy to make the index match.

A plano-concave lens may also be used with the same approach. However in this way there will be a hole between the covered lens and the plexiglass. Therefore, we preferred the first system. Spherical mirrors have aberration problems. The defect that all mirrors in spherical shapes have prohibits the mirror from focusing all the incident light from the same location. For light rays striking the outer edges of the mirror this problem is more noticeable because these rays fail to focus in the same exact point as the rays strike the inner part of the mirror. This defect may cause blurriness.

Using an ellipsoidal mirror prevents this aberration effect. The most challenging part of this thesis was to fabricate a convenient ellipsoidal mirror. Three different methods were attempted to find a good solution as explained in Chapter 3. The best results were obtained when the ellipsoidal mirror is fabricated via diamond turning. FOV of 70 degrees is achieved with this design. A laser vs LED comparison was also made during this work. The image with the laser has better resolution than the LED source but is corrupted with speckle noise.

BIBLIOGRAPHY

[1]“DLP Technology for Near Eye Display.” Texas Instruments http://www.vuzix.com/augmented-reality/ Accessed 3 September 2015

[2] Azuma, Ronald, et al. "Recent advances in augmented reality." Computer Graphics and Applications, IEEE 21.6 (2001): 34-47.

[3] Furht, Borko, ed. Handbook of augmented reality. Springer Science & Business Media, 2011.

[4] Sensorama simulator. U.S. Patent No 3,050,870, 1962.

[5] Sutherland, Ivan E. "A head-mounted three dimensional display." Proceedings of the December 9-11, 1968, fall joint computer conference, part I. ACM, 1968.

[6] “Google Glass ancestors: 45 years of digital eyewear.” CNET http://www.cnet.com/pictures/google-glass-ancestors-45-years-of-digital-eyewear-photos/16/ Accessed 8 September 2015

[7]O. Cakmakci, J. Rolland. Head-worn displays: a review. Journal of Display Technology, 2006, 2.3: 199-216.

[8] https://www.oculus.com/en-us/rift/ Accessed 15 August 2015

[9]Pölönen, M., T. Järvenpää, and J. Häkkinen. "Comparison of near-to-eye displays: subjective experience and comfort." Journal of display technology 6.1 (2010): 27-35

[10]Hua, Hong, and Bahram Javidi. "A 3D integral imaging optical see-through head-mounted display." Optics express 22.11 (2014): 13484-13491.

[11]http://www.vuzix.com/augmented-reality/

[12].http://innovega-inc.com/how-it-compares.php

[13]Lanman, Douglas, and David Luebke. "Near-eye light field displays." ACM Transactions on Graphics (TOG) 32.6 (2013): 220.

[14]Järvenpää, Toni, and Viljakaisa Aaltonen. "Compact near-to-eye display with integrated gaze tracker." Photonics Europe. International Society for Optics and Photonics, 2008.
[15]Järvenpää, Toni, and Monika Pölönen. "P-33: Measurements of a Prototype See-through Near-eye Display with Diffractive Light Guides." SID Symposium Digest of Technical Papers. Vol. 43. No. 1. Blackwell Publishing Ltd, 2012.
[16] DUE, BRIAN. "CHALLENGES WITH GOOGLE GLASS IN SOCIAL INTERACTION." 4TH PARTICIPATORY INNOVATION CONFERENCE 2015.
[17]Maimone, Andrew, et al. "Pinlight displays: wide field of view augmented reality eyeglasses using defocused point light sources." ACM SIGGRAPH 2014 Emerging Technologies. ACM, 2014.
[18]http://innovega-inc.com/new-architecture.php
[19] Fahri Yaraş, Hoonjong Kang, and Levent Onural, "Circular holographic video display system," Opt. Express 19, 9147-9156 (2011)
[20] Choi, Chil-Sung, et al. "Ultra-slim coherent backlight unit for mobile holographic display." SPIE Nanoscience+ Engineering. International Society for Optics and Photonics, 2015.
[21] Yuan Xiong, Zhenghong He, Chao Ping Chen, Xiao Li, Ang Li, Zhicheng Ye, Jiangang Lu, Gufeng He, Yikai Su, Coherent backlight system for flat-panel holographic 3D display, Optics Communications, Volume 296, 1 June 2013, Pages 41-46, ISSN 0030-4018,
[22] Shariv, I., Yaakov Amitai, and A. A. Friesem. "Compact holographic beam expander." Optics letters 18.15 (1993): 1268-1270.
[23] Gulanyan, É. Kh. "Holography with an extended reference-beam source."Quantum Electronics 1.4 (1972): 355-361.

[24] Stroke, George W., and Robert C. Restrick III. "Holography with spatially noncoherent light." Applied Physics Letters 7.9 (1965): 229-231.
[25] Chang, Byung Jin. "Holography with non-coherent light." Optics Communications 9.4 (1973): 357-359.
[26] Ghatak, Ajoy. "The Optical Fiber: A Historical Perspective." Journal of Optics33.3 (2004): 131-143.
[27] Al-Azzawi, Abdul. Fiber optics: principles and practices. CRC Press, 2006., 5-10
[28] Issa, Nader A. "High numerical aperture in multimode microstructured optical fibers." Applied optics 43.33 (2004): 6191-6197.
[29] Hulst, Hendrik Christoffel, and H. C. Van De Hulst. Light scattering by small particles. Courier Corporation, 1957.
[30] Jahnke, James A. Continuous emission monitoring. John Wiley & Sons, 2000
[31] Driggers, Ronald G., Melvin H. Friedman, and Jonathan Nichols. Introduction to infrared and electro-optical systems. Artech House, 2012.
[32] Tilley, RJ.D. 2004. Scattering In: Understanding Solids: The Science of Materials. Published by John Wiley and Sons:452-455.
[33] Luther, Wolfgang, Axel Zweck. "Safety Aspects of Engineered Nanomaterials." CRC Press (2013) 17-18
[34] Dewaker Varun,"Nanoparticles: A Revolution to Biology" (2014) Biotech Express Vol 1 Issue 7
[35] Chen, Xiaobo, and Samuel S. Mao. "Titanium dioxide nanomaterials: synthesis, properties, modifications, and applications." Chemical reviews 107.7 (2007): 2891-2959.
[36] Rastar, Amir, et al. "Theoretical Review of Optical Properties of Nanoparticles."Journal of Engineered Fabrics & Fibers (JEFF) 8.2 (2013).
[37] Krasnikov, I., et al. "Influence of titanium dioxide nanoparticles on skin surface temperature at sunlight irradiation." Biomedical optics express 2.12 (2011): 3278-3283.

[38] Taylor J, Lynch C., Dlugos J. F.,“Particle Characterization of UV Blocking Sunscreens and Cosmetics Using UV/Visible Spectroscopy” PerkinElmer, Inc. Shelton, CT, Technical Note, 2013
[39] Boronat, T., et al. "Influence of temperature and shear rate on the rheology and processability of reprocessed ABS in injection molding process." Journal of Materials Processing Technology 209.5 (2009): 2735-2745.
[40] Biron, Michel. Thermoplastics and thermoplastic composites. William Andrew, 2012.
[41] Oraby, Samy E., and Ayman M. Alaskari. "Atomic force microscopy (AFM) topographical surface characterization of multilayer-coated and uncoated carbide inserts." Microscopy (Image data type:“Friction”) 33 (2010): 38.
[42] http://www.technologystudent.com/equip1/inject1.htm